

An Empirical Study on Writer Identification & Verification from Intra-variable Individual Handwriting

Chandranath Adak^{a,b}, Bidyut B. Chaudhuri^c, Michael Blumenstein^a

^aCentre for AI, School of Software, University of Technology Sydney, Australia - 2007

^bIIS, School of ICT, Griffith University, Gold Coast, Australia - 4222

^cCVPR Unit, Indian Statistical Institute, Kolkata, India - 700108

Abstract

The handwriting of an individual may vary substantially with factors such as mood, time, space, writing speed, writing medium and tool, writing topic, etc. It becomes challenging to perform automated writer verification/identification on a particular set of handwritten patterns (e.g., speedy handwriting) of a person, especially when the system is trained using a different set of writing patterns (e.g., normal speed) of that same person. However, it would be interesting to experimentally analyze if there exists any implicit characteristic of individuality which is insensitive to high intra-variable handwriting. In this paper, we study some handcrafted features and auto-derived features extracted from intra-variable writing. Here, we work on writer identification/verification from offline Bengali handwriting of high intra-variability. To this end, we use various models mainly based on handcrafted features with SVM (Support Vector Machine) and features auto-derived by the convolutional network. For experimentation, we have generated two handwritten databases from two different sets of 100 writers and enlarged the dataset by a data-augmentation technique. We have obtained some interesting results.

Keywords: Intra-variable handwriting, Writer identification, Writer verification.

1. Introduction

“Handwriting” is basically a kind of pattern. However, from the pre-historic era, it bears the connotation of human civilization. The handwriting instrument progressed from finger and wedge (on clay/sand and stone-based medium) to quill, pencil, fountain/ball-point pen (on parchment, papyrus/paper), and again finger (on the touch-screen of a smart device). Though the world is going fast towards a paperless e-world, “handwriting remains just as vital to the enduring saga of civilization (–Michael R. Sull)”.

For computer scientists, *automated analysis of handwriting* is a recognized field of study owing to the ever-increasing complexity of extreme variations and having positive impacts on the fields of Forensics, Biometrics, Library Science and Data Science.

Email addresses: chandranath.adak@uts.edu.au (Chandranath Adak), bbcisical@gmail.com (Bidyut B. Chaudhuri), michael.blumenstein@uts.edu.au (Michael Blumenstein)

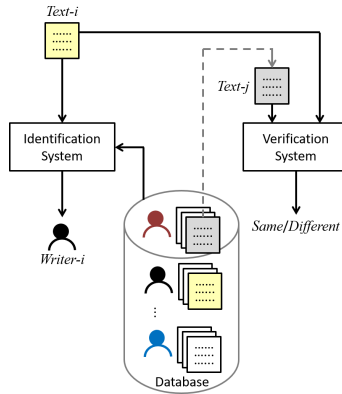


Figure 1: Ideal writer identification and verification system.

The handwriting pattern varies with person due to individual writing style. This may be termed as *inter-class variance*. It is also noted that handwriting samples of a single person may vary extensively with various factors such as mood, time, space (geographical location), writing medium and tool. This is referred to as *intra-class variance*. Sometimes, these inter-class and intra-class variations are termed as “between-writer” and “within-writer” variability, respectively [43]. Even for excessive stroke variation among handwritten specimens of a particular writer, the writer and others having long exposure to his/her writing may still recognize it. Some implicit stroke characteristics may be the reason behind this ability.

In the field of forensics and biometrics, verifying/identifying a writer from a handwriting sample is sometimes essential (e.g., in the case of the “2001 anthrax attacks”). Now-a-days, computer-assisted automated analysis is also quite popular in this application. Writer verification is a task used to authenticate a given document whether it is written by a certain individual or not. In writer identification, the goal is to match the writers to their handwriting specimens. The target of the writer identification/verification task is to maximize inter-variability and to minimize intra-variability.

The workflow of writer identification and verification approach is shown in Fig. 1. Here, we have a database of handwritten texts with its known authors/writers. A query text sample $Text-i$ is input to the writer identification system to obtain its writer-id ($Writer-i$) as an output with a certain degree of accuracy where the database provides support for the retrieval. In the writer verification system, two text samples $Text-i$ and $Text-j$ are fed to decide whether they are written by the “Same” or “Different” persons. The $Text-i$ is a query sample to be verified and the $Text-j$ may be fed from the database of known authors.

In the document image analysis literature, interest has grown in the area of automated writer identification/verification for the last four decades. A detailed survey of the reported research works on this topic up to the year 1989 have been compiled in [51]. Recent advancements on writer identification/verification can be found in [55, 68]. Most of the past research work [51, 55, 68] has focused on ideal handwriting generated in normal circumstances without paying much attention to the intra-variability.

However, a situation may arise where an author needs to be verified based on a quickly

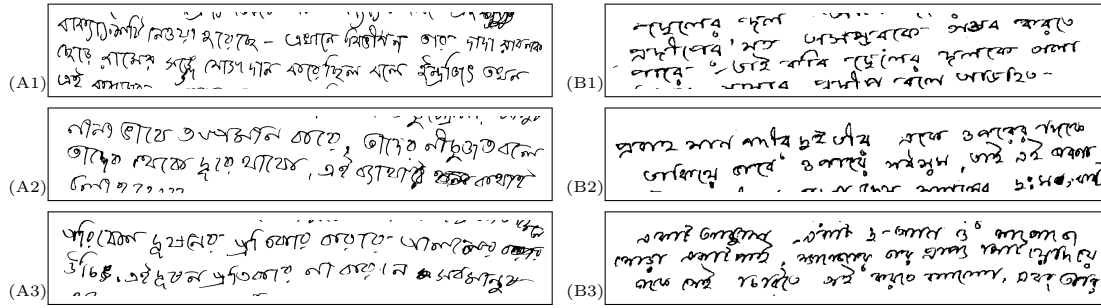


Figure 2: Intra-variable Bengali handwritten samples, *left column*: (A1), (A2), (A3) samples are of Writer-A, *right column*: (B1), (B2), (B3) samples are of Writer-B. The intra-variability of Writer-A’s samples is less compared to Writer-B’s samples, as confirmed by handwriting experts.

written, unadorned handwritten manuscript, whereas only regular neat/clean handwriting with known authorship is available in the training database. Similar situations may occur where we need to identify the writer from unclaimed tidy handwriting, but the available database contains only careless untidy writing. In such a situation, the available writing of the person in the database and the test document written by the same individual can be highly dissimilar. In Fig. 2, two sets of intra-varied handwritten sample of two individual writers are shown. Here, for example, we may need to verify whether the sample of Fig. 2.(B1) is written by Writer-B, on the basis of B’s handwriting of say Fig. 2.(B3).

In this paper, we focus on the situation of intra-variation of individual handwriting to perform writer identification/verification. Ideally, within-writer variation should be less than the between-writer variation, which is the basis of the writer identification/verification task [43]. However, where the intra-variation is relatively higher (refer to Fig. 2), we need to find some handwriting features less sensitive to intra-variability and more sensitive to inter-variability.

We have generated two sets of database of intra-variable handwriting to deal with such realistic scenarios of writing identification/verification. Our database contains offline handwriting of *Bengali* (endonym, *Bangla*) script which is a fairly complex Indic script and used by more than 250 million people [49, 10]. Recent advancements in writer identification on Indic scripts have been reported in [13]. The general features of Bengali script can be found in [10]. In connection with writer identification, some useful characteristics of Bengali handwriting are mentioned in [13], for example, matra/headline, delta, hole, coil shape, etc. We have noted that these Bengali handwriting characteristics along with classical handwriting characteristics (inter-text-line and inter-word gap, text-line skew, word/character slant, height/width of a character, text main-body height, character formation, etc.) usually vary with writing.

In our generated database, the intra-variation is relatively higher than most of the existing databases in the literature [68], as confirmed by some handwriting experts. Therefore, here, we need to find some handwriting features which can decrease the intra-variability and increase the inter-variability.

The *applicability* of this work is as follows. *First*, it will be helpful in the fields of forensics and biometrics for writer identification and verification. *Second*, this work studies the impact of working with absent data, i.e., when a particular type of individual writing

is absent in the training set, how the system performs while testing with that type. *Third*, this work may be useful in some applications of cultural heritage and library science. When some unpublished manuscripts of a scholar are found, the authorship is usually verified [32]. Now, for the case of newly-discovered manuscripts, if they contain some unknown writing styles of the scholar, our work may provide some insights to analyze the authorship. *Fourth*, this work may have a modest understanding of the progress of some diseases such as Parkinson’s, Alzheimer’s, Dysgraphia, Dyslexia, Tourette syndrome, etc., which affect handwriting. Here, before and after the disease progression, handwritten specimens have high intra-variability and provide some applicability of our work.

In this paper, we analyze the intra-variable handwriting for writer identification and verification tasks. The writer identification task is perceived as an n -class classification problem to classify handwritten documents in n number of writer classes. On the other hand, writer verification is perceived as a binary classification, where a document is marked with “Same” or “Different” class, if it is written by the *same* or *different* writer of the given document, respectively. For these tasks, we extract two types of features, handcrafted and auto-derived [42], from an offline handwritten text sample set. Then the extracted features are classified to identify/verify a writer. In writer identification, SVM (*Support Vector Machine*) is used for handcrafted features and some deep neural models are used for auto-derived features. In writer verification, we employ some similarity metrics on handcrafted and auto-derived features.

Our *contribution* to this paper is the study of writer identification/verification on the intra-variable handwriting of an individual. Such a rigorous investigation is the earliest attempt of its type. For this study, we have generated two databases containing intra-variable handwriting in a controlled and uncontrolled way. The subgrouping of the uncontrolled database with respect to intra-variability is rather new. Here, the handwritten pages of the uncontrolled database are initially clustered with some deep features, and then finally grouped by confirmation of a classification technique which is pre-trained by the controlled database. We also propose two patch selection tactics to provide the input to the deep architectures without any normalization. Moreover, two writer identification strategies are introduced here, which are relatively new. The data augmentation technique is also a new addition here with respect to the offline handwritten data.

The rest of the paper is organized as follows. Section 2 discusses related work and Section 3 describes the experimental dataset generation procedure. Then Section 4 mentions the preprocessing step before entering into the methodology. After that Section 5 and Section 6 describe the handcrafted and auto-derived feature extraction techniques, respectively. The writer identification procedure is discussed in Section 7, followed by Section 8 with a description of the writer verification process. The subsequent Section 9 is comprised of experimental results and discussions. Finally, Section 10 concludes this paper.

2. Related Work

With our both online and offline searching capacities, we have not found any direct work on intra-variable handwriting for writer identification/verification. In this section, at first, we cite some slightly related works mentioning intra-variability in handwriting.

Then we briefly discuss some interesting work on writer investigation (i.e., identification/verification).

2.1. Intra-variability in Handwriting

The handwriting of a person may change for using various writing instruments. The handwriting alteration of a person using a pen and pencil has been studied in [31]. Hilton [46] reported that some pens can suppress the writing characteristics of an individual and may introduce intra-variability.

The handwriting of a person may change with the writing surface, more precisely, by the friction between the writing medium (paper) and tool (pen). Gerth et al. [54] studied this within-writer variability when writing was performed on paper and a tablet computer.

Handwriting also changes with time span and the age of a person [39, 35]. Speedy writing in excitement, or writing with a stressed mind may degrade the writing quality, thus produces within-writer variability [39, 6].

Some diseases such as Parkinson's, Alzheimer's, etc. affect the handwriting of an individual [35, 28]. Therefore, before and after such diseases, the writing shows intra-variability.

Alcohol consumption also changes the individual's writing style and provides an example of intra-variable handwriting [22].

Such *mechanical* (e.g., writing instrument, surface, etc.), *physical* (e.g., illness, aging, etc.), *psychological* (e.g., excitement, anger, mood, etc.) factors may cause large individual handwriting variation [39].

2.2. Writer Investigation

The root of writer analysis can be found around 1000 B.C. when a few Japanese scholars studied the bar formation in writing to judge personal characteristics [53]. However, with the boom of automation, during the late 20th century, such investigations had also started to be automated. In the beginning of the 21st century, the "9/11 attacks" and "2001 anthrax attacks" have escalated automated writer identification/verification research.

In the document image analysis domain, automated writer investigation research is being performed during the last four decades. Plamondon and Lorette [51] surveyed major works in this field up to the year 1989. After that, the offline writer investigation research up to the year 2007, is described in [43]. The recent advancements in this field can be found in [68]. The writer investigation research work on Indic scripts is discussed in [13]. However, most of the past research has dealt with ideal handwriting without degradation [51, 43, 68]. But, a handwritten page may contain various artifacts such as struck-out/crossed-out writing [15, 9, 1], doodles [12], ruled lines, printed text, logos, stamps, etc. [30].

Chen et al. [30] studied the impact of ruled line removal on writer identification. They [30] showed that the performance improved by retaining, instead of deleting the ruled lines. Another work in [15] reported the effect of struck-out texts on writer identification. The authors [15] experimentally showed that the presence of struck-out texts in a handwritten document degrades the writer identification performance. A preliminary work on crossed-out text removal with its effect on writer identification is presented in [1].

Instead of handwritten text, sometimes writer inspection has been performed on unconventional notations such as musical scores [3], sketches [27], etc.

In the literature, writer identification has been tried with training on one script and testing on another [17, 14]. In [17], English and Greek scripts were used, while in [14], English and Bengali scripts were reported.

3. Experimental Dataset

For our experimental analysis, we needed a database of intra-variable handwritten samples of each writer. We did not find any such publicly available database. Therefore, we had to generate a new database containing such handwriting specimens. We made two offline databases on the basis of a handwriting collection strategy, namely *controlled* and *uncontrolled* databases.

3.1. Controlled Database (D_c)

In this case, all volunteers chosen for supplying data were aware of the modality of our experiments. For controlled database collection, we focused on intra-variability occurring mostly due to writing speed [36]. It is noted that typically speedy writing is more distorted than the usual handwriting of a writer, and this inference was confirmed by some handwriting experts.

Collecting previously written samples at various speeds from many writers is quite challenging, since no one typically monitors and records his/her writing speed unless required for a specific reason. Therefore, we collected handwriting under a controlled setup, as follows.

All volunteers were instructed to write at various speeds. At first, they were advised to write at their normal speed of writing. Then they were instructed to write faster than their normal writing speed. Finally, they were requested to write at a slower speed than normal. We labelled these as *medium* (or, normal), *fast*, and *slow* sets of handwriting samples, respectively.

At the stage of full-page writing, we noted the total time (t) of writing using a stop-watch and computed the total length (l) of writing strokes on a page. The handwriting speed (s) in a full page is calculated as stroke length per unit time, i.e., $s = l/t$. The stroke length is computed from counting the number of object pixels from the thinned version of the writing strokes. For thinning purpose, the *Zhang-Suen thinning* method [61] was used which worked better than some other techniques [41]. Additionally, in the thinned version, a spurious branch having length less than half of the average stroke-width is pruned.

The reaction time (≈ 200 millisecond) [5] for using a stop-watch is negligible with respect to the objective of our task. We prepared our experimental setup to write on a white 70 GSM (g/m^2) A4 page and placing it on a horizontally plane surface with a smooth ball-point pen having black/blue ink. We created our database in offline mode, and did not use any digital pen/surfaces which could obstruct the individual writing habits. Here, our primary aim is to capture the intra-variability of handwriting, on which our technique can work adequately without using accurate, ultramodern speed measuring instruments.

For a writer W_i , a fast handwritten page is chosen where handwriting speed (s_i , a scalar quantity) is greater than a threshold $T1_i$, i.e., $s_i > T1_i$. For slow handwriting, $s_i < T2_i$, where $T2_i$ is another threshold. The medium handwritten page is chosen where $T1_i \geq s_i \geq T2_i$. The medium or normal handwriting speed is captured at first from multiple handwritten pages of a writer W_i . We calculate mean (μ_{si}) and standard deviation (σ_{si}) of medium speed from these pages. Here, we use $T1_i = \lceil \mu_{si} + \alpha_s \cdot \sigma_{si} \rceil$ and $T2_i = \lceil \mu_{si} - \alpha_s \cdot \sigma_{si} \rceil$. We set $\alpha_s = 2$, which is decided empirically.

Each writer wrote multiple pages which were ordered in terms of the writing speed. We chose top speedy two pages from the *fast* handwritten samples, two lowest-speeded pages from the *slow* writing, and middle-speeded two pages from the *medium* writing.

Although many volunteers contributed for our database generation, we chose 100 writers whose handwriting patterns varied structurally due to writing speeds, as advised by some handwriting experts. This is performed in order to generate a database of intra-variable handwriting.

The writers were native Bengali from West Bengal, India. The finally selected 100 writers were in the age group of 12-42 years having academic backgrounds from secondary school to university level. The ratio of male to female writers in this database is 14:11.

This controlled dataset (D_c) contains 600 pages where each writer contributed 6 pages of Bengali handwriting. Among 6 pages, 2 pages are of *fast* handwriting speed, 2 pages are of *medium* and the remaining 2 pages are of *slow* speed. In other words, we have 3 sets of handwriting namely S_f (*fast*), S_m (*medium*), S_s (*slow*), each containing 2 handwritten pages of every 100 writers.

3.2. Uncontrolled Database (D_{uc})

For generation of the uncontrolled database, the writers should be unaware of our experiments before the data collection. However, people generally perform their daily writing at a normal pace using various pens and papers, and a uniform data collection setup is missing. Here, we came up with a different strategy for this type of database generation.

After discussions with some handwriting experts, we note that in real-life school examinations, the students generally write at various speeds, since the examination time is limited and the usual target is to score good marks by answering all questions within that stipulated period. Therefore, the students/writers are in a hurry when the clock is ticking towards the end of exam. However, here some behavioral/psychological aspects [7, 36] may influence intra-variable handwriting, besides the writing-speed, due to anxiety, nervousness to finish, panic of a low score, stress to recollect the answer, etc.

Therefore, we have selected a real school-exam scenario to collect suitable data by maintaining uniformity for this data collection. Some details of such situation are as follows:

- i) *Time*: The examination duration was fixed as three hours. Here, the time works as a constraint to ascertain the increase/decrease of writing speed and individual variability.
- ii) *Question type*: We selected a 100-mark Bengali literature examination paper, where most of the question types were broad subjective to be answered in many sentences.
- iii) *Script*: The answers were to be written in Bengali script.

iv) *Paper*: For writing the answers, white pages of 70 GSM (g/m^2) with a fixed size of $215.9 \times 355.6 \text{ mm}^2$ were provided.

v) *Pen*: The writers used their own pens. Most of the pens were of black/blue ink with 0.5 - 1.0 mm ball-point tip.

vi) *Writer*: The writers were native Bengali from West Bengal, India, and students of VIII - XII grade Bengali-medium public schools. Their age ranged between 13 - 19 years. All these writers were different from the volunteers participated in controlled database generation.

The exam marking was performed by school teachers. For our task, we chose the answer script of a student who scored at least 40% and wrote at least 6 full pages. A total of 153 writers were chosen in this way. Among these writers, 67 persons wrote 6 pages each, 11 persons wrote 7 pages each, 54 persons 8 pages each, 21 persons 9 pages each. Therefore, 153 writers contributed a total of 1100 pages.

Now, we have 1100 unlabelled pages of 153 writers. We label each page in one of the 3 groups of intra-variable writings, say, S'_{fa} , S'_{ma} and S'_{sa} . For this grouping, at first, we use auto-derived feature-based clustering techniques, as follows.

We use the front part of GoogLeNet [19] for feature extraction, since this architecture provides encouraging accuracy with comparatively lesser dimension of feature vector [44]. From each page, an n_p number of text-patches of size 224×224 is chosen arbitrarily. This n_p is set empirically to 400. For each patch, we have obtained 1024-dimensional deep feature vector from the *avg pool* layer of GoogLeNet [19]. For clustering, we choose various clustering algorithms such as K-means, Fuzzy C-means, Minibatch K-means, Expectation-Maximization with Gaussian-Mixture-Models (EM with GMM), and Agglomerative Hierarchical Clustering (Agglo_Hierarchical) [2].

Let us assume that p_{ij} denotes $\text{patch}_i \mid i = 1, 2, \dots, 400$ of $\text{page}_j \mid j = 1, 2, \dots, 1100$. Actually, p_{ij} represents a 1024-dimensional feature vector obtained from patch_i of page_j . For p_{1j} , we obtain a cluster plot CL_1 by patch_1 's of all the 1100 pages. Similarly, cluster plot CL_2 is obtained from patch_2 's of all 1100 pages. And so on, patch_{400} 's of all 1100 pages produce cluster plot CL_{400} . These 400 cluster plots are ordered with a corresponding patch; i.e., patch_i 's (or, the i^{th} patch) of all pages produce CL_i . Moreover, we obtain 600 (fixed empirically) cluster plots unordered with patches which are chosen arbitrarily. Therefore, we now have 1000 ($= 400 + 600$) cluster plots. Each cluster plot contains 1100 patches (i.e., patch-based feature points), where each patch represents each of the 1100 pages. From these 1000 cluster plots, using the *majority rule*, we label each page into three groups/clusters S'_{fa} , S'_{ma} and S'_{sa} . For example, suppose in all the 1000 cluster plots, majority of the patches of page_1 (p_{i1}) fall in the cluster S'_{fa} ; then the page_1 is put into the group S'_{fa} .

To find which clustering algorithm among K-means, Fuzzy C-means, Minibatch K-means, EM with GMM, and Agglo_Hierarchical, would work well for intra-variable handwriting, we use an external evaluation criterion, called NMI (*Normalized Mutual Information*) score [16]. For this, we perform a similar feature extraction strategy and clustering techniques on the controlled dataset D_c , which contains the ground-truth. Employing various clustering techniques on D_c , we have obtained the NMI scores, as presented in Table 1. The Agglo_Hierarchical method worked well on D_c , so we use this clustering

Table 1. Clustering method evaluation on D_c

Clustering method	NMI score
K-means	0.637
Minibatch K-means	0.610
Fuzzy C-means	0.646
EM with GMM	0.679
Agglo.Hierarchical	0.684

technique here also on uncontrolled data.

Up to this point, the 1100 unlabelled pages of 153 writers are clustered into 3 groups (S'_{fa} , S'_{ma} and S'_{sa}) using an unsupervised clustering technique (Agglo_Hierarchical).

Now, we classify the 1100 pages into 3 classes (S'_{fb} , S'_{mb} and S'_{sb}) supervised by the controlled database D_c . For this classification, we use GoogLeNet due to its promising performance in other computer vision related tasks [19]. Here also, we arbitrarily choose n_p (= 400, fixed empirically) number of text patches in a page and input to the GoogLeNet. A page is classified into a certain class where the majority of its patches fall.

To assess the efficiency of the GoogLeNet on intra-variable handwriting, we perform a 3-class classification experiment on D_c to classify in S_f , S_m , S_s sets/classes due to having the appropriate ground-truth. For this, we divide D_c into training, validation, and test sets in the ratio of 2:1:1. The performance on the test set of D_c for this 3-class classification problem is 96.87%, which is quite satisfactory for our task.

For classification of uncontrolled handwritten samples (1100 pages), we perform training on the entire controlled database D_c and test on these 1100 pages. After this classification, we have obtained the members of 3-classes S'_{fb} , S'_{mb} and S'_{sb} .

Our intention is to generate 3 sets (S'_f , S'_m and S'_s) of samples containing intra-variable handwriting of an individual. Therefore, each of these 3 sets must contain handwriting samples of every writer.

From the unsupervised clustering, we obtain S'_{fa} , S'_{ma} and S'_{sa} sets. From supervised classification, we get the sets S'_{fb} , S'_{mb} and S'_{sb} . From 153 writers, we choose a certain writer who has at least 2 handwriting samples in each of the S'_{fa} , S'_{ma} , S'_{sa} sets and the same 2 samples in each of the corresponding S'_{fb} , S'_{mb} , S'_{sb} sets. Finally, these 3×2 samples of a writer are put in S'_f , S'_m and S'_s sets, respectively. Out of 153 writers, this constraint is successfully satisfied by 104 writers. Furthermore, we take advice from some handwriting experts and finally choose 100 writers from the 104 writers.

Our uncontrolled database (D_{uc}) contains 3 sets (S'_f , S'_m and S'_s) of intra-variable handwriting samples of 100 writers. Each of the S'_f , S'_m and S'_s sets contain 2 samples per writer. Therefore, similar to the controlled database D_c , this uncontrolled database D_{uc} also contains 600 pages in total. The ratio of male to female writers in D_{uc} is 31:19.

In this uncontrolled database, we observe that the handwriting of most students becomes structurally more distorted and unadorned in the latter pages of the answer booklet.

4. Preprocessing

All the handwritten pages were scanned by a flat-bed scanner at 300 ppi (*pixels per inch*) in 256 gray-values to obtain digital document images. In the preprocessing stage, we label the components of a handwritten document image using a relatively faster single-pass

connected component labeling algorithm [25]. The text region is extracted after removal of the non-text components if present any, using the method of [12]. In the text region, the struck-out texts are also deleted by employing the method of [9], since the presence of struck-out text impedes the usual writer identification performance [15]. However, the style of strike-out strokes [9] may be utilized for writer inspection, which is out of the scope of our current work. Very small sized components such as dots, dashes, commas, colons etc., and noise are also removed. The text-lines and words are segmented using an off-the-shelf 2D Gaussian filter-based method *GOLESTAN-a*, as discussed in [45]. Character level segmentation is also performed using a water reservoir principle-based method [62].

5. Handcrafted Feature Extraction

A writer identification task can be viewed as a multi-class classification problem, where the task is to assign the writer-id to the unknown handwritten specimens. Similarly, writer verification can be perceived as a binary classification problem where the task is to answer *yes/no* to a questioned handwritten sample as to whether it has been written by a particular writer. The features used for these tasks are described in this section and the following section. We employ both handcrafted features and auto-derived features [42]. Handcrafted features are required to be predesigned explicitly in the traditional way, whereas auto-derived features do not have any explicit design.

The extracted handcrafted features are discussed as follows.

5.1. Macro-Micro Features (F_{MM})

The macro and micro features of Srihari et al. [59] are quite popular since those were very effective in writer identification from handwritings of 1500 U.S. population having various ethnic groups/ages/genders. Here, we adopt this set of features for our task.

Initially, we choose the macro feature vector, described in [59], which contains 11 features: gray-level entropy (f_1), gray-level threshold (f_2), count of black pixels (f_3), interior/exterior contour connectivity (f_4 - f_5), vertical/negative/positive/horizontal contour slope (f_6 - f_9), average slant and height of the text-line (f_{10} - f_{11}). From [59], we note that the features f_1 , f_2 , and f_3 are related to the pen pressure. Here, f_4 and f_5 reveal the writing movement. The features f_6 , f_7 , f_8 , and f_9 are related to stroke formation. The feature f_{10} represents the writing slant and f_{11} is related to the text proportion.

Two paragraph-level macro features are also considered: height to width ratio of a paragraph, i.e., aspect ratio (f_{12}) and margin width (f_{13}). Three more word-level macro features are also employed, which are upper zone ratio (f_{14}), lower zone ratio (f_{15}) and length (f_{16}). We calculate these paragraph and word-level features over a page and take the average value.

The character-level micro features contain 192-bit gradient, 192-bit structural and 128-bit concavity features, concatenated into a 512-bit feature. The detailed description of these features can be found in [59]. We modify this micro feature slightly to get a page-level feature vector. From a page, we obtain the histogram of this 512-bit feature and normalize it by the character count.

The macro and micro features are concatenated to generate the feature vector F_{MM} .

5.2. Contour Direction and Hinge Features (F_{DH}):

For writer identification, stroke direction and curvature-based features have been reported to work well [51, 68]. Therefore, we use here the famous contour direction and hinge distribution of handwritten strokes proposed by Bulacu and Schomaker [43].

Along the writing stroke contour, an angle (ϕ) histogram is generated and normalized into a probability distribution $p_f(\phi)$. From the horizontal direction, the angle (ϕ) is calculated as:

$$\phi = \tan^{-1} \frac{y_{i+\epsilon} - y_i}{x_{i+\epsilon} - x_i}; \quad (1)$$

where, x_i and y_i denote the row and column indices of the i^{th} object pixel. The ϵ depends on stroke-thickness and is fixed as 5 in [43]. In our task, ϵ (> 1) is data-driven, and worked well for $\epsilon = \max(2, \lfloor \mu_{sw} - \sigma_{sw} \rfloor)$, where μ_{sw} is the average stroke-width and σ_{sw} is the standard deviation of stroke-width in a page. The number of histogram bins (n_b) is set as 12 within the range of $0^\circ - 180^\circ$. Hence, 15° per bin is engaged. Clearly, the dimension of this feature $p_f(\phi)$ or f_{cd} is 12.

In [43], for the contour hinge feature f_{ch} , two contour fragments, joined to a common end, making angles ϕ_1 and ϕ_2 (where, $\phi_2 \geq \phi_1$), spanning all four quadrants (360°), are considered. A normalized histogram is generated with a joint probability distribution $p_f(\phi_1, \phi_2)$. Similar to [43], the number of histogram bins (n_b) is set to 12, leading to $n_b(2n_b + 1) = 300$ -dimensional feature vector.

By concatenating f_{cd} and f_{ch} , we obtain F_{DH} .

5.3. Direction and Curvature Features at Keypoints (F_{DC})

We intend to ascertain some similarities between handwriting specimens of an individual. Therefore, we focus on some points of interest, i.e., *keypoints* (ρ_i), on the handwritten strokes. These keypoints are obtained by combining some structural points (i.e., start/end, branch and curved points) and SIFT (*Scale-Invariant Feature Transform*) keypoints on Bengali handwritten ink-strokes, as described in [13].

Here, our plan is to observe the movement of writing strokes on these keypoints, and therefore, we capture the stroke direction and curvature at the keypoints. For *direction* and *curvature* feature extraction from *offline* handwritten strokes, we use the idea of ‘‘The NPen++ Recognizer’’ [58] which deals with *online* handwriting.

We calculate the writing *direction* between two connected keypoints ρ_i and ρ_{i+1} in terms of Cosine and Sine values and use them as features f_{dc} and f_{ds} , respectively.

$$f_{dc} \equiv \cos(\theta_i) = \frac{\rho_{i+1}.x - \rho_i.x}{d_i} \quad (2)$$

$$f_{ds} \equiv \sin(\theta_i) = \frac{\rho_{i+1}.y - \rho_i.y}{d_i} \quad (3)$$

where, $\rho_i.x$ and $\rho_i.y$ are the row and column indices of ρ_i , and $d_i = \sqrt{(\rho_{i+1}.x - \rho_i.x)^2 + (\rho_{i+1}.y - \rho_i.y)^2}$.

The *curvature* of a writing stroke is the angle made by the line fragments $\overline{\rho_{i-1} \rho_i}$ (from ρ_{i-1} to ρ_i) and $\overline{\rho_i \rho_{i+1}}$ (from ρ_i to ρ_{i+1}). The Cosine and Sine values of this angle are calculated and employed as features f_{cc} and f_{cs} , respectively.

$$f_{cc} \equiv \cos(\theta_i - \theta_{i-1}) = \cos\theta_i \cos\theta_{i-1} + \sin\theta_i \sin\theta_{i-1} \quad (4)$$

$$f_{cs} \equiv \sin(\theta_i - \theta_{i-1}) = \sin\theta_i \cos\theta_{i-1} - \cos\theta_i \sin\theta_{i-1} \quad (5)$$

For each of these four features (f_{dc} , f_{ds} , f_{cc} , f_{cs}), we generate separate normalized histograms spanning the range of $[-1, 1]$ for a number of bins $n_b = 200$. Therefore, the dimension of each feature vector is 200.

Concatenating features f_{dc} , f_{ds} , f_{cc} and f_{cs} , we get F_{DC} .

6. Auto-derived Feature Extraction

The auto-derived features are mainly extracted using a convolutional neural network (CNN). The convolutional architecture generally contains two parts: front and rear. The front part typically extracts the features. The rear part is used for classification (refer to Section 7.2).

The front part of the CNN takes an input image. We use some patch-based strategies to feed fixed sized input images [63]. Here, we do not use any image normalization, since it impedes the writer identification performance [8]. The patch selection is not performed through the classical sliding-window technique, since the text-lines are not skew-normalized. Sliding a window horizontally through the middle of the text-line (main text-body height) is conceivable, but the information may be lost for several cases such as for highly skewed text-lines, for overlapping text-lines with lesser inter-text-line gaps, etc.

Here, two types of patches are selected as follows.

(a) *patch_{char}*: We already have the character-level information from the pre-processing stage. We find the center of gravity (p_{CG}) of a segmented character image. Then we take a $n_{char} \times n_{char}$ window centering the p_{CG} , and consider it as a character-level patch, say *patch_{char}*.

(b) *patch_{allo}*: We have obtained some keypoints on writing strokes, as mentioned in Section 5.3. A neighboring window of size $n_{allo} \times n_{allo}$ centered at a keypoint is used as a patch. This patch is an allographic-level patch, say *patch_{allo}*.

From a text sample, all the *patch_{char}*s and *patch_{allo}*s are extracted. Each *patch_{char}* is fed to the front part of the CNN and a feature vector f_{pc} is obtained. Similarly, for each *patch_{allo}*, a feature vector f_{pa} is generated.

In our task, the following deep-learning architectures are used separately for *patch_{char}* and *patch_{allo}* as inputs.

6.1. Basic_CNN

The LeNet-5 is a celebrated convolutional network that works well on various machine learning problems [69]. Our Basic_CNN architecture is primarily influenced by this LeNet-5 and provides an initial flavor of a deep learning model for our task. Here, we use 3 convolutional layers (C_i), each followed by a sub-sampling (max-pooling, MP_i) layer. The

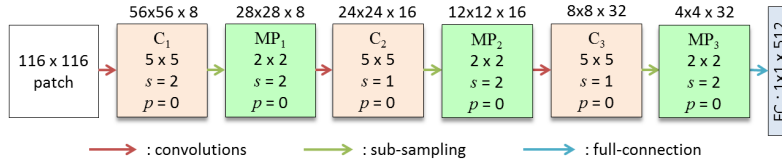


Figure 3: $\text{BCNN}_{\text{char}}$: Basic_CNN architecture as a feature extractor while using $\text{patch}_{\text{char}}$.

used feature map count with map size, filter size, stride (s), padding (p) values are shown in Fig. 3. For example, the first convolutional layer (C_1) contains 8 feature maps of size 56×56 each, and each feature map is connected to a 5×5 neighbor window of the input. Here, $s = 2$ and $p = 0$ is used. For each convolutional layer, instead of the \tanh activation function of LeNet-5, we use ReLU (*Rectified Linear Unit*) [65] due to its advantages of sparsity and reduced likelihood of vanishing gradient.

For feature extraction using both $\text{patch}_{\text{char}}$ and $\text{patch}_{\text{allo}}$, the used Basic_CNN architectures ($\text{BCNN}_{\text{char}}$ and $\text{BCNN}_{\text{allo}}$) are almost similar except some minor differences. The $\text{patch}_{\text{char}}$ size is $n_{\text{char}} \times n_{\text{char}}$, and $\text{patch}_{\text{allo}}$ size is $n_{\text{allo}} \times n_{\text{allo}}$. Here, $n_{\text{allo}} = \lfloor n_{\text{char}}/2 \rfloor$ is used. We fix the n_{char} as 116. For feeding $\text{patch}_{\text{char}}$ in the first convolutional layer (C_1) of $\text{BCNN}_{\text{char}}$, $s = 2$ and $p = 0$ are used. However, for C_1 of $\text{BCNN}_{\text{allo}}$, $s = 1$ and $p = 1$ are employed. The rest of the $\text{BCNN}_{\text{allo}}$ architecture is kept similar to $\text{BCNN}_{\text{char}}$ (refer to Fig. 3). In this case, we use *Stochastic Gradient Descent* (SGD) as optimizer with $\text{initial_learning_rate} = 0.01$, $\text{momentum} = 0.9$, and $\text{weight_decay} = 0.0005$. The other parameters of Basic_CNN are similar to the LeNet-5 [69].

Employing this Basic_CNN, we obtain a feature vector of size 512 for each patch.

6.2. SqueezeNet

The AlexNet [4] is one of the pioneering models of deep learning revolution and the winner of ILSVRC (*ImageNet Large Scale Visual Recognition Challenge*)-2012 [47]. The recent deep learning era has been started from AlexNet [44]. For our task, we employ some major deep learning architectures, discussed here and the following subsections.

The SqueezeNet architecture provides AlexNet-level accuracy with lesser parameters and a reduced demand on memory [24]. Therefore, we use SqueezeNet here, instead of AlexNet. The details of the SqueezeNet can be found in [24], and we use the *Simple Bypass* version of this network. Here, we call the layers by their names as used in [24]. For our task, we use the same weights trained on ImageNet [47, 4] by adopting the concept of *transfer learning* [57].

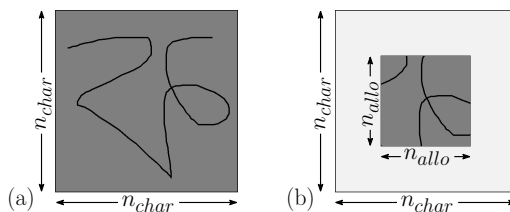


Figure 4: (a) $\text{patch}_{\text{char}}$ of size $n_{\text{char}} \times n_{\text{char}}$, (b) $\text{patch}_{\text{allo}}$ of size $n_{\text{allo}} \times n_{\text{allo}}$ is shown in dark-gray, and the zero-padding, bounding the $\text{patch}_{\text{allo}}$ is shown in light-gray color.

We select $n_{char} \times n_{char}$ sized $patch_{char}$ and $n_{allo} \times n_{allo}$ sized $patch_{allo}$ to be fed separately to the SqueezeNets (SN_{char} and SN_{allo}), where $n_{allo} = \lfloor n_{char}/2 \rfloor$. The SqueezeNet takes a standard input of fixed size, i.e., 224×224 . Here, n_{char} equals to 224 and consequently, n_{allo} becomes 112. Therefore, we use a zero-padding of width 56 ($= \lfloor (n_{char} - n_{allo})/2 \rfloor$) to the boundary of $patch_{allo}$, as shown in Fig. 4, for maintaining the standard input size of SqueezeNet.

After the *conv10* and *avgpool10* (refer to [24]) layer of SqueezeNet, we obtain a 100 (number of writers)-sized feature vector for each patch.

6.3. GoogLeNet

We choose this network, since it won the ILSVRC-2014 [47] competition and obtained a performance closer to human-being. The details of this architecture can be found in [19]. This GoogLeNet architecture is also called as *Inception V1*. We employ two separate GoogLeNets (GN_{char} and GN_{allo}) to feed $patch_{char}$ and $patch_{allo}$. The input patch size is similar to the SqueezeNet. The size of $patch_{char}$ is 224×224 and $patch_{allo}$ is 112×112 . Here also, $patch_{allo}$ is bound by a zero-padding of width 56. The rest of the GN_{char} and GN_{allo} architectures are similar to the GoogLeNet of [19]. The weights are transferred by pre-training of GoogLeNet using ImageNet data.

After the *avg pool* layer [19], a 1024-dimensional feature vector can be obtained.

6.4. Xception Net

The refined versions of GoogLeNet (*Inception V1*) [19] are *Inception V2* [56] and *Inception V3* [20]. Also, the Xception Net [23] is a stronger version of the *Inception V3*. Therefore, we use this Xception Net (with two fully connected layers). The name ‘‘Xception’’ is coined from ‘‘Extreme Inception’’.

The $patch_{char}$ fed Xception Net (XN_{char}) takes $n_{char} \times n_{char}$ sized input images and follows the architecture of [23]. Xception Net [23] takes 299×299 sized input image. Therefore, we use $n_{char} = 299$. A separate Xception Net (XN_{allo}) is used to feed $patch_{allo}$ of size $n_{allo} \times n_{allo}$. Here, we use $n_{allo} = \lfloor n_{char}/2 \rfloor = 149$. Since, Xception Net takes fixed sized input of 299×299 , a zero-padding of width 75 ($= \lfloor (n_{char} - n_{allo})/2 \rfloor$) is employed here, similar to the scheme used for SqueezeNet (refer to Section 6.2, Fig. 4). The pre-trained Xception Net on ImageNet data by the transfer learning [23] is used here with the same weights.

We obtain a 2048-dimensional feature vector from the *GlobalAveragePooling* layer [23] of both XN_{char} and XN_{allo} .

6.5. VGG-16

The VGG architecture was the runner-up of the competition ILSVRC-2014. We choose the 16 layers’ VGG architecture due to its simplicity and uniformity in convolutions. The detail of this architecture is reported in [40].

We use two VGG-16 networks (VN_{char} and VN_{allo}). The VGG-16 takes a fixed size input of 224×224 . Therefore, we input 224×224 sized $patch_{char}$ to the VN_{char} . Similar to the SqueezeNet, here also, we use 112×112 sized $patch_{allo}$ with 56 pixel wide zero-padding to feed to the VN_{allo} . Otherwise, VN_{allo} and VN_{char} networks are the same, and follow the architecture of VGG-16 pre-trained on ImageNet data [40].

After the *FC-4096* layer [40], we obtain a 4096-dimensional feature vector from each of VN_{allo} and VN_{char} .

6.6. ResNet-101

This architecture won ILSVRC-2015 and beat human-level performance on ImageNet data [47]. Although ResNet is very deep, it is faster and has fewer parameters compared to the VGG network. The novelty of the ResNet (*Residual Network*) is its residual or skip connections. The details of this architecture can be found in [38] and we use the ResNet with 101 layers. Here, we use two such nets (say, RN_{char} and RN_{allo}).

The ResNet also takes fixed sized, i.e., 224×224 input. Therefore, we feed 224×224 sized $\text{patch}_{\text{char}}$ as input to the RN_{char} . Similar to the SqueezeNet, we feed 112×112 sized $\text{patch}_{\text{allo}}$ with zero-padding of width of 56 to the RN_{allo} (refer to Section 6.2). The rest of the RN_{allo} is similar to the RN_{char} , and both of them follow the architecture of ResNet-101 as reported in [38]. The weights are transferred by pre-training on ImageNet database [47, 38].

For each of the RN_{char} and RN_{allo} , we obtain a 2048-dimensional feature vector after the *avg pool* layer [38].

7. Writer Identification

As discussed earlier in Section 1, the writer identification problem is a multi-class classification problem, where the number of classes is equal to the total count of writers.

7.1. Handcrafted Feature-based Identification

The handcrafted feature vector obtained from a text sample is fed to an SVM classifier to mark the text sample to its writer-id. The SVM generally works well for multi-class classification in a wide range of pattern recognition applications [70]. With regards to the SVM-based multi-class classification for handwriting-related tasks, the *one-against-all* strategy works better than the *one-against-one* [33]. It can also be noted from [18, 9] that the SVM with an RBF (*Radial Basis Function*) kernel [64] works better than some other classifiers such as k-NN (*k-Nearest Neighbors*), MLP (*Multi-Layer Perceptron*), MQDF (*Modified Quadratic Discriminant Function*) and SVM-linear for Abjad (Farsi), Alphabetic (English) and Abugida (Bengali) handwritings. Hence, we use the one-against-all SVM-RBF for our task.

The SVM-RBF hyper-parameters \mathcal{C} and γ are essential to be tuned to avoid overfitting and to regulate the decision boundary, respectively [37]. For optimal performance of the classifier, the hyper-parameters are selected from a tuning set. We use the traditional grid-searching technique for this purpose [64]. A suitable value for \mathcal{C} is chosen at first from a range of values by cross-validation and then several γ 's are tested from a range of values for better \mathcal{C} 's.

The best performance is obtained for $\mathcal{C} = 2^2$ within the range $[2^{-3}, 2^{-2}, \dots, 2^6]$ and $\gamma = 2^4$ within the range $[2^{-3}, 2^{-2}, \dots, 2^8]$. Here, 5-fold cross-validation is used.

7.2. Auto-derived Feature-based Identification

From the text samples, writers are classified using the rear part of the convolutional neural architectures.

For Basic_CNN, the rear classifier part is actually an MLP with 1 hidden layer containing 256 nodes, set empirically. The output layer’s nodes depict the number of writer classes.

The rear part of SqueezeNet, GoogleNet, Xception Net, VGG-16, ResNet-101 are used for writer identification (classification). The rear parts of the SqueezeNet, GoogleNet, Xception Net, VGG-16, ResNet-101 commence after the *avgpool10* [24], *avg pool* [19], *GlobalAveragePooling* [23], *FC-4096* [40], *avg pool* [38] layers, respectively. All these respective rear part classifiers follow their original architecture [24, 19, 23, 40, 38].

We have obtained the features from multiple patches of a handwritten page. Now, to identify a writer on a whole page, the following two strategies are used. The inputs of the classifiers are also based on the following two strategies.

(a) *Strategy-Major*: On the basis of feature vector (f_{pi}) extracted from each patch (p_i), we classify the writer (W_{pi}) individually on each patch. In other words, we label each of the multiple patches of a page with a writer-id.

Next, we apply *majority rule* to find the ultimate writer (W) of the page. For example, on a page, if the majority of the text patches are marked with writer-A, then the overall page is considered as written by writer-A. This strategy is presented in Algorithm 1.

(b) *Strategy-Mean*: The individual feature vector (f_{pi}) obtained from each of the patches (p_i) of a page is extracted. Here, we calculate the arithmetic mean (m_{pi}) of a feature vector (f_{pi}) obtained from each patch (p_i). Therefore, for each patch (p_i), we have a single scalar mean value (m_{pi}). From the mean values of all patches, we generate a mean feature vector (m_p) for a page. This mean feature vector is used to classify a page into

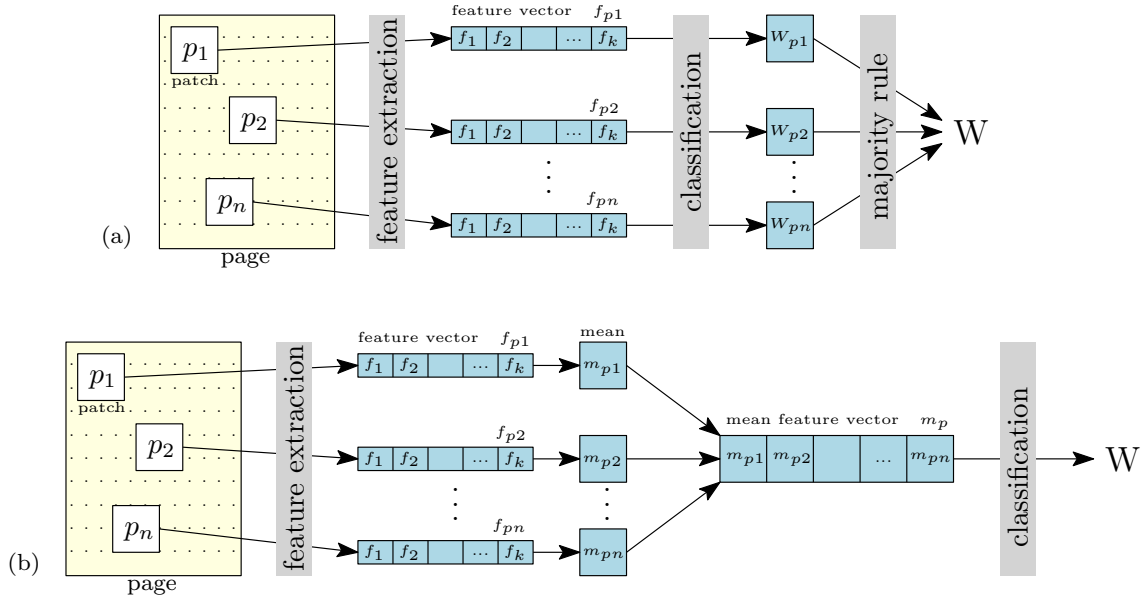


Figure 5: Writer identification strategies: (a) *Strategy-Major*, (b) *Strategy-Mean*.

Algorithm 1 *Strategy-Major*

1: Input: $f_{p1}, f_{p2}, \dots, f_{pn}$ | feature vectors of patches p_1, p_2, \dots, p_n in a page;
2: Output: W | writer of the page;
3: **for** $i = 1, 2, \dots, n$ **do** $\triangleright n :=$ number of patches
4: $W_{pi} = \text{classify}(f_{pi});$ $\triangleright W_{pi} :=$ writer of patch p_i
5: **end for**
6: W = majority ($W_{p1}, W_{p2}, \dots, W_{pn}$);

writer class (W). In Algorithm 2, we present this strategy.

Algorithm 2 *Strategy-Mean*

1: Input: $f_{p1}, f_{p2}, \dots, f_{pn}$ | feature vectors of patches p_1, p_2, \dots, p_n in a page;
2: Output: W | writer of the page;
3: **for** $i = 1, 2, \dots, n$ **do** $\triangleright n :=$ number of patches
4: $m_{pi} = \text{arithmeticMean}(f_{pi});$
5: **end for**
6: $m_p = \{m_{p1}, m_{p2}, \dots, m_{pn}\};$ $\triangleright m_p =$ feature vector of m_{pi} 's
7: W = classify (m_p);

For easy and quick understanding, *Strategy-Major* and *Strategy-Mean* are diagrammatically represented in Fig. 5.

Two types of patches $\text{patch}_{\text{char}}$ and $\text{patch}_{\text{allo}}$ (refer to Section 6) are used in both *Strategy-Major* and *Strategy-Mean* for writer identification.

8. Writer Verification

In this section, we discuss the writer verification task using handcrafted features followed by auto-derived features.

8.1. Handcrafted Feature-based Verification

In the writer verification task, we check whether two handwriting specimens are written by the same person or not. In fact, the goal is to find some distance measure between the two handwritten samples. If this distance is greater than a *decision threshold* T , then we infer that the samples are different, and the same, otherwise ($\leq T$) [34].

The distance measure is calculated using the handcrafted features generated from the handwritten sample. We used several distance measures such as *Minkowski* up to *order* 5 (*Manhattan* when the *order* = 1, *Euclidean* when *order* = 2), *Bhattacharya*, *chi-square* (χ^2) and *Hausdorff* [11]. Here the chi-square (χ^2) distance worked well for our purpose.

The chi-square distance (χ_{ij}^2) between features obtained from two handwritten samples, i.e., *sample-i* and *sample-j*, are calculated as follows:

$$\chi_{ij}^2 = \sum_{n=1}^N \frac{(f_{in} - f_{jn})^2}{(f_{in} + f_{jn})}; \quad (6)$$

where, f_{in} and f_{jn} are the feature vectors obtained from *sample-i* and *sample-j*, respectively. N denotes the dimension of the feature-vector and n represents the index.

In this writer verification task, two types of error are considered: *False Accept (FA)* and *False Reject (FR)*. The nomenclatures of these errors depict their definition. *FA* is an error when two documents are falsely accepted as having the “same” source (written by the same writer), though actually they are “different”. *FR* is the error when two documents are falsely rejected as “different” (written by different writers), when in fact they are written by the “same” person.

The error rates *FAR* (*False Acceptance Rate*) and *FRR* (*False Rejection Rate*) are calculated empirically by integration (up to/from the decision threshold T) of the distribution of distances between handwritten samples from different person $P_D(x)$ and the distribution of distances between samples of same person $P_S(x)$, respectively [43].

$$FAR = \int_0^T P_D(x)dx , \quad FRR = \int_T^\infty P_S(x)dx . \quad (7)$$

From *FAR* versus *FRR* plot, we obtained the *EER* (*Equal Error Rate*) where $FAR = FRR$. The writer verification performance in terms of *accuracy* is obtained as $(1 - EER) \times 100\%$.

8.2. Auto-derived Feature-based Verification

The Siamese Net [29] performs well for weakly supervised similarity metric learning and is successfully applied on various computer vision tasks, e.g., face verification [52], person re-identification [21], geo-localization [60], etc. Therefore, we use this net for writer verification using auto-derived features. Here, our task is treated as a binary classification to classify two handwritten specimens into “same” or “different” sourced.

Siamese Net contains identical twin neural architectures to produce two feature vectors from two images to be compared (Fig. 6) [52, 60]. The neural networks of Section 6 are used for Siamese twins. Here, employing the *Strategy-Mean* of Section 7.2, we obtain the mean feature vector from a handwritten page H_i , considered as one subnet of the Siamese twins. Parallel to this, another mean feature vector is obtained by the other subnet of the Siamese twins from one more handwritten page H_j to be compared with H_i . These twin architectures of the Siamese Net are joined by a *loss function* (L) at the top to train the similarity metric from the data. In this case, we use a margin-based loss function, i.e., *contrastive loss function* [50], which is given by:

$$L(H_i, H_j, l) = \alpha(1 - l)D_w^2 + \beta l \{\max(0, m - D_w)\}^2 ; \quad (8)$$

where, *label* $l = 0$, if H_i and H_j are matched as the same, and $l = 1$, otherwise. Two constants α and β are chosen empirically as $\alpha = 0.5$ and $\beta = 0.5$. The margin $m > 0$ is set as the average squared pair distance. $D_w \equiv D_w(H_i, H_j) = \|f(H_i) - f(H_j)\|_2$ is the Euclidean distance between $f(H_i)$ and $f(H_j)$ which are two feature vectors generated by mapping of H_i and H_j to a real vector space through the convolutional network.

For performance evaluation, a threshold d is used on D_w to verify whether two handwritten samples are written by the “same” or a “different” writer. All the handwriting pairs (H_i, H_j) , inferred to be written by the same writer are denoted as \mathcal{P}_{same} , whereas all pairs written by different writers are denoted as \mathcal{P}_{diff} .

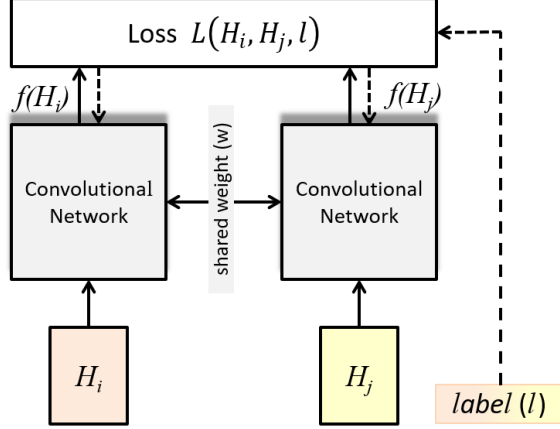


Figure 6: Siamese architecture.

Now, we define the set of true positives (TP) at d as follows:

$$TP(d) = \{(H_i, H_j) \in \mathcal{P}_{same}, \text{ with } D_w(H_i, H_j) \leq d\} ; \quad (9)$$

where all the handwriting pairs are correctly classified as the “same”.

Similarly, when all the handwriting pairs are correctly classified as “different”, then the set of true negatives (TN) at d is defined as:

$$TN(d) = \{(H_i, H_j) \in \mathcal{P}_{diff}, \text{ with } D_w(H_i, H_j) > d\} . \quad (10)$$

The true positive rate (TPR) and true negative rate (TNR) at d are computed as:

$$TPR(d) = \frac{|TP(d)|}{|\mathcal{P}_{same}|} , \quad TNR(d) = \frac{|TN(d)|}{|\mathcal{P}_{diff}|} . \quad (11)$$

The overall accuracy is calculated as:

$$Accuracy = \max_{d \in D_w} \frac{TPR(d) + TNR(d)}{2} , \quad (12)$$

by varying d in the range of D_w with a step of 0.1.

For writer verification, we use page-level auto-derived features obtained from both patch types $patch_{char}$ and $patch_{allo}$, using *Strategy-Mean* of Section 7.2.

9. Experiments and Discussions

In this section, at first, we discuss the database employed and the data augmentation for its distribution among the training, validation and test sets. Then we present the results of writer identification and verification.

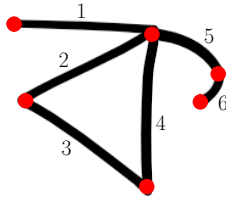


Figure 7: Pictorial representation of a Bengali character component: keypoints are marked by red dots and the six edges are numbered from ‘1’ to ‘6’.

9.1. Database

As mentioned in Section 3, we have generated controlled (D_c) and uncontrolled (D_{uc}) databases, comprised of 600 pages each. D_c contains 3 sets (S_f , S_m , and S_s) of intra-variable writing. Each of these 3 sets contains 2 handwritten pages of 100 writers. Likewise, D_{uc} contains 3 sets S'_f , S'_m and S'_s , each having 2 pages by another set of 100 writers.

For intensive experimentation, we need to augment our dataset. The data augmentation technique used here is presented below.

9.1.1. Data Augmentation

For augmenting our dataset, we are influenced by the idea of “*DropStroke*” [66] that is inspired by “Dropout” method from the deep neural network [26]. In [66], the *DropStroke* method is used to generate new data by omitting some strokes randomly from an *online* handwritten Chinese character.

Here, the *offline* data lacks the advantage of stroke drawing information of online data. However, we remodel the *DropStroke* as per our requirement for offline handwriting. We use the keypoint information here (refer to Section 5.3). The ink-pixel connection between two consecutive keypoints is considered as an edge/path/stroke. We drop one edge from a text component (i.e., mostly character, obtained in Section 4) in such a strategy, so that the number of connected components does not increase. Thus, in Fig. 7, edge ‘1’ or ‘5’ or ‘6’ cannot be dropped since it will generate extra component; all the remaining edges can be dropped without any violation of this strategy.

To generate new samples from a page, we drop $\lceil \alpha_d \cdot n_d \rceil$ number of edges arbitrarily subject to the above condition. Here, n_d is the number of characters in a page and α_d is a parameter in a range of [0.1, 1], set empirically. The value of n_d is computed in Section 4.

Initially, a handwritten page is roughly horizontally split into two half-pages, which is a common technique for expansion of data samples in the writer identification task [67]. From each of these two half pages, we generate 10 different samples using our data augmentation technique. Therefore, a handwritten page produces 2 half-pages and 20 ($= 2 \times 10$) augmented handwritten samples, i.e., overall 22 ($= 2 + 20$) text samples (refer to Fig. 8).

Thus, each of the databases D_c and D_{uc} contains 13200 ($= 600 \text{ pages} \times 22 \text{ samples}$) text samples. Now, each of the subsets S_f , S_m , S_s and S'_f , S'_m , S'_s contains 44 ($2 \text{ pages} \times 22 \text{ samples}$) text samples from each of the 100 writers.

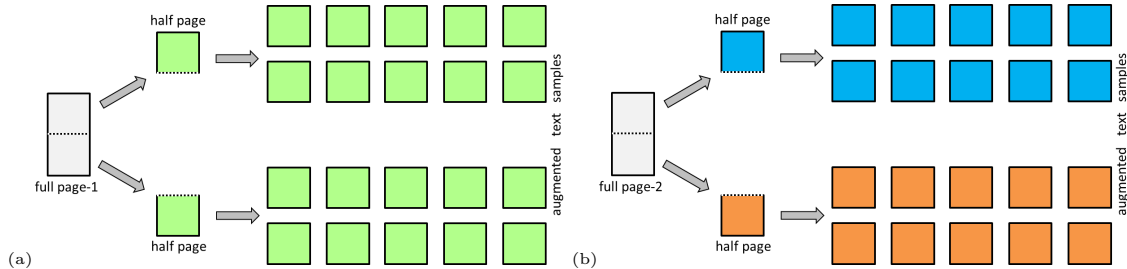


Figure 8: Augmented text samples, generated from 2 handwritten pages of a writer in set S_f . The subset S_{f1} contains green colored 22 samples for training, S_{f2} contains blue colored 11 samples for validation, and S_{f3} contains orange colored 11 samples for testing.

We divide both databases D_c and D_{uc} into training, validation, and test sets with a 2:1:1 ratio. The set S_f is divided into S_{f1} (training), S_{f2} (validation) and S_{f3} (test) subsets. The S_{f1} , S_{f2} , S_{f3} contains 22, 11, 11 text samples, respectively, from each of the 100 writers. We have ensured distinctiveness among training, validation and test sets, so that no common data is in between any pair of these sets. More elaborately, the S_{f1} contains 22 text samples generated from the full *page-1* of a writer in S_f . The subset S_{f2} contains 11 samples obtained from the top-half of the full *page-2*, and S_{f3} contains 11 samples generated from the bottom-half of this *page-2*. This is diagrammatically represented in Fig. 8 for easy understanding. In this case, $S_f = S_{f1} \cup S_{f2} \cup S_{f3}$. Similarly, S_m , S_s and S'_f , S'_m , S'_s sets are divided into training, validation and test sets. Here, $S_m = S_{m1} \cup S_{m2} \cup S_{m3}$, $S_s = S_{s1} \cup S_{s2} \cup S_{s3}$; $S'_f = S'_{f1} \cup S'_{f2} \cup S'_{f3}$, $S'_m = S'_{m1} \cup S'_{m2} \cup S'_{m3}$, $S'_s = S'_{s1} \cup S'_{s2} \cup S'_{s3}$.

Now, for our writer identification/verification task, we train and test with various types of intra-variable data. The experiments are performed in this way to imitate real-life situations, where a particular type of handwriting may be absent (refer to Section 1).

9.2. Writer Identification Performance

In this subsection, we discuss the performance of the writer identification models based on handcrafted features and auto-derived features.

The writer identification accuracy is computed using a “Top- N ” criterion, where the correct writer is marked at least one time within the ‘ N ’ (\ll total number of writers) top-most classifier output confidences. Here, we compute results of Top-1, Top-2, and Top-5 criteria. However, Top-1 accuracies are presented in more detail for comparison among models. Top-2 and Top-5 accuracies are also presented when a better outcome is achieved.

9.2.1. Writer Identification Performance with Handcrafted Features

Here, we discuss the writer identification performance on both databases, D_c and D_{uc} , by employing handcrafted features.

9.2.1.1. Writer Identification by Handcrafted Features on D_c .

The Top-1 writer identification performance on database D_c by employing feature F_{MM} with SVM classifier (say, system “ $WI_{D_c-F_{MM}}$ ”) is shown in Table 2.

Table 2. Top-1 writer identification performance of system $WI_D_c-F_{MM}$

Set		Accuracy (%)		
	Test	S_{s3}	S_{m3}	S_{f3}
Training				
S_{s1}		61.23	37.17	29.49
S_{m1}		38.45	60.48	36.67
S_{f1}		31.45	34.59	59.32
$S_{s1} + S_{m1}$		61.42	61.89	37.04
$S_{s1} + S_{f1}$		62.24	38.47	60.33
$S_{m1} + S_{f1}$		40.72	60.95	59.86
$S_{s1} + S_{m1} + S_{f1}$		62.78	62.23	61.31

Table 3. Top-1 writer identification performance of system $WI_D_c-F_{DH}$

Set		Accuracy (%)		
	Test	S_{s3}	S_{m3}	S_{f3}
Training				
S_{s1}		72.67	44.71	37.29
S_{m1}		45.53	71.86	44.17
S_{f1}		39.23	43.59	70.93
$S_{s1} + S_{m1}$		72.92	72.84	44.85
$S_{s1} + S_{f1}$		72.86	45.42	71.54
$S_{m1} + S_{f1}$		46.28	72.37	71.72
$S_{s1} + S_{m1} + S_{f1}$		73.49	73.36	72.26

Here, by training with all the training data ($S_{s1} + S_{m1} + S_{f1}$) of D_c , and testing only on S_{s3} , we obtain a 62.78% accuracy. Likewise, training on $S_{s1} + S_{m1} + S_{f1}$, and testing on S_{m3} and S_{f3} , we obtain 62.23% and 61.31% accuracies, respectively.

Experimenting on the same type set yields better accuracy, e.g., training on subset S_{s1} and testing on subset S_{s3} (say, experimental setup S_{s1}/S_{s3} or, E_{ss}) provides 61.23% accuracy, where both training and testing are parts of the set S_s . Similarly, experimental setup S_{m1}/S_{m3} (E_{mm}) and S_{f1}/S_{f3} (E_{ff}) provides a 60.48% and 59.32% accuracy, respectively.

Next, we look at the performance of experiments on different training and test sets. For example, training on S_{s1} and testing on S_{m3} (say, experimental setup S_{s1}/S_{m3} or, E_{sm}) yields 37.17% accuracy, which is quite low. The reverse experimental setup, i.e., S_{m1}/S_{s3} (E_{ms}) also shows poor performance (38.45% accuracy). Similarly, experimental setups E_{mf} , E_{fm} , E_{sf} , E_{fs} provide poor results, with accuracies 36.67%, 34.59%, 29.49%, 31.45%, respectively. The reason behind such a low outcome is the presence of high variability between the training and test sets. Experimental setups E_{sf} and E_{fs} show the lowest performance, since they contain highly intra-variable writing.

For our task, we define the performance of our model by a tuple of 9 major accuracies (%) obtained by various experimental setups. This 9-tuple is $(AE_{ss}, AE_{mm}, AE_{ff}, AE_{smv}, AE_{sfv}, AE_{mfv}, AE_{smf/s}, AE_{smf/m}, AE_{smf/f})$ which is used to compare multiple models used in this paper. AE_{ss} , AE_{mm} , AE_{ff} are the accuracy measures obtained from the E_{ss} , E_{mm} , E_{ff} experimental setups, respectively. These AE_{ss} , AE_{mm} , AE_{ff} accuracies show the efficacy of a model on low intra-variable handwriting, which are mostly similar types. In Table 2, we show these accuracies highlighted in **green**, which can be seen better in the softcopy of this paper.

AE_{smv} is the average (arithmetic mean) accuracy obtained from experimental setups E_{sm} (S_{s1}/S_{m3}) and E_{ms} (S_{m1}/S_{s3}). This is depicted with **red** shade in Table 2. Similarly, AE_{sfv} is obtained from E_{sf} , E_{fs} (**blue** shaded in Table 2) and AE_{mfv} is obtained from E_{mf} , E_{fm} (**yellow** in Table 2), respectively. AE_{smv} , AE_{sfv} , AE_{mfv} demonstrate the system performance when both training and test sets contain highly intra-variable writing.

$AE_{smf/s}$ is the accuracy obtained from the experimental setup $E_{smf/s}$, where training is performed on $S_{s1} + S_{m1} + S_{f1}$, and testing is executed on S_{s3} . $AE_{smf/m}$ and $AE_{smf/f}$ are obtained by testing on S_{m3} and S_{f3} , respectively, while training is performed on $S_{s1} + S_{m1} + S_{f1}$, similar to the training of $AE_{smf/s}$. Here, $AE_{smf/s}$, $AE_{smf/m}$, $AE_{smf/f}$ show the performance when the system is trained with all available handwriting varieties of an individual. In Table 2, we show these accuracies in **gray** shade.

The performance of the system $WI_D_c-F_{MM}$ in terms of 9-tuple is (61.23, 60.48, 59.32,

37.81, 30.47, 35.63, 62.78, 62.23, 61.31).

The Top-1 writer identification performance on database D_c using feature F_{DH} with SVM (say, system “ $WI_{D_c-F_{DH}}$ ”) is shown in Table 3. The performance of system $WI_{D_c-F_{DH}}$ in terms of 9-tuple is (72.67, 71.86, 70.93, 45.12, 38.26, 43.88, 73.49, 73.36, 72.26). This can be tallied with Table 3, as we tallied $WI_{D_c-F_{MM}}$ performance with Table 2.

The Top-1 writer identification performance on database D_c using feature F_{DC} with SVM (say, system “ $WI_{D_c-F_{DC}}$ ”) is shown in Table 4. The performance of system $WI_{D_c-F_{DC}}$ in terms of 9-tuple is (71.54, 70.25, 69.71, 43.56, 36.38, 40.80, 72.48, 71.85, 70.93). This can be tallied with Table 4.

Table 4. Top-1 writer identification performance of system $WI_{D_c-F_{DC}}$

Set	Test	Accuracy (%)		
		S_{s3}	S_{m3}	S_{f3}
Training				
S_{s1}		71.54	43.20	37.04
S_{m1}		43.92	70.25	41.06
S_{f1}		35.72	40.54	69.71
$S_{s1} + S_{m1}$		71.75	70.84	41.74
$S_{s1} + S_{f1}$		71.66	43.37	70.14
$S_{m1} + S_{f1}$		44.47	71.45	70.68
$S_{s1} + S_{m1} + S_{f1}$		72.48	71.85	70.93

Table 5. Top-1 writer identification performance using handcrafted features on D_c

Model	9-tuple Accuracy (%)									Rank
	AE_{ss}	AE_{mm}	AE_{ff}	AE_{smv}	AE_{sfv}	AE_{mfv}	$AE_{smf/s}$	$AE_{smf/m}$	$AE_{smf/f}$	
$WI_{D_c-F_{MM}}$	61.23	60.48	59.32	37.81	30.47	35.63	62.78	62.23	61.31	3
$WI_{D_c-F_{DH}}$	72.67	71.86	70.93	45.12	38.26	43.88	73.49	73.36	72.26	1
$WI_{D_c-F_{DC}}$	71.54	70.25	69.71	43.56	36.38	40.80	72.48	71.85	70.93	2

Combining Tables 2, 3 and 4, we generate Table 5 to present only the 9-tuple accuracies of all handcrafted feature-based writer identification models dealing with D_c , for comparison and easy visualization.

The models are ranked using the *Borda count* [48]. Here, the models are initially ranked with respect to each accuracy of the 9-tuple (i.e., performance on each experimental setup), then the aggregate ranking is computed by the *max* rule. If there is a draw between two models, then we provide weightage on the accuracies AE_{smv} , AE_{sfv} , AE_{mfv} . The aggregate ranks are shown in the last columns of Tables 5 - 8. Here, Rank ‘1’ denotes first, i.e., the best performing model, Rank ‘2’ indicates the second best performing model, and so on.

Although, we have computed 21 accuracy measures as in Tables 2 - 4, we present the 9-tuple accuracy measures like Table 5 further for model assessment and for simple visualization.

9.2.1.2. Writer Identification by Handcrafted Features on D_{uc} .

By employing database D_{uc} , here also, we generate three similar handcrafted feature-based writer identification models as mentioned in Section 9.2.1.1. In Table 6, we present the performance of these models on D_{uc} with respect to the 9-tuple accuracy.

In this case, while employing D_{uc} , the AE_{ss} accuracy is obtained from an experimental setup E_{ss} where S'_{s1} is used for training and S'_{s3} is used for testing. Similarly, for obtaining $AE_{smf/m}$, training is performed on $(S'_{s1} + S'_{m1} + S'_{f1})$, and testing is executed on S'_{m3} . Likewise, other accuracies of 9-tuple are obtained (refer to Section 9.2.1.1).

Table 6. Top-1 writer identification performance using handcrafted features on D_{uc}

Model	9-tuple Accuracy (%)									Rank
	AE_{ss}	AE_{mm}	AE_{ff}	AE_{smv}	AE_{sfv}	AE_{mfv}	$AE_{smf/s}$	$AE_{smf/m}$	$AE_{smf/f}$	
$WI_{D_{uc}}-F_{MM}$	60.08	58.51	57.72	37.01	29.77	33.92	61.63	61.04	60.01	3
$WI_{D_{uc}}-F_{DH}$	71.79	71.21	70.19	43.85	37.01	42.21	72.93	72.66	71.97	1
$WI_{D_{uc}}-F_{DC}$	69.77	68.69	68.54	42.43	34.96	39.16	70.82	70.02	69.66	2

Experimenting on both the databases D_c and D_{uc} using handcrafted features, overall the F_{DH} feature-based model performed the best and the F_{MM} feature-based model achieved the lowest results.

It can be observed from Tables 5 and 6 that the accuracies AE_{smv} , AE_{sfv} , AE_{mfv} are very low. We have noted on AE_{smv} , AE_{sfv} , AE_{mfv} , even Top-2 (Top-5) writer identification performance provides additional at most 0.38% (2.97%) and 0.30% (2.53%) accuracy on D_c and D_{uc} , respectively.

9.2.2. Writer Identification Performance with Auto-derived Features

We perform writer identification by feeding $\text{patch}_{\text{char}}$ to the Basic_CNN with the *Strategy-Major*, and call this model: “BCNN_char_major”. Likewise, feeding $\text{patch}_{\text{char}}$ to the Basic_CNN with the *Strategy-Mean*, is called a “BCNN_char_mean” model. The $\text{patch}_{\text{allo}}$ s when input into the Basic_CNN with the *Strategy-Major* and the *Strategy-Mean*, are called the “BCNN_allo_major” and the “BCNN_allo_mean”, respectively.

Thus, a convolutional network produces 4 variations of auto-derived feature-based models for writer identification, i.e., “x_char_major”, “x_char_mean”, “x_allo_major”, and “x_allo_mean”. Here, ‘x’ is to be replaced by the convolutional network name. The ‘x’ is replaced by ‘SN’, ‘GN’, ‘XN’, ‘VN’, ‘RN’ while employing SqueezeNet, GoogLeNet, Xception Net, VGG-16, ResNet-101, respectively. For example, feeding $\text{patch}_{\text{char}}$ in GoogLeNet with the *Strategy-Mean* is called: “GN_char_mean”.

Consequently, 6 types of convolutional networks, each of 4 various configurations, produce a total of 24 ($= 6 \times 4$) models. Here, we present the previously mentioned 9-tuple accuracy measure for each model (refer to Section 9.2.1.1).

9.2.2.1. Writer Identification by Auto-derived Features on D_c .

In Table 7, we present the 9-tuple writer identification accuracies of auto-derived feature-based models performing on the D_c database.

The ranks of the models are shown in the rightmost column of the Table 7. Here, the XN_allo_mean model performed best for writer identification on the D_c database. Although in this model, the AE_{ss} , $AE_{smf/s}$ accuracies are more than 97%, the performance is comparatively lower with respect to AE_{smv} , AE_{sfv} , AE_{mfv} accuracies.

In Table 7, the overall *Strategy-Mean* worked better than *Strategy-Major*. In general, the $\text{patch}_{\text{allo}}$ with the *Strategy-Mean* worked better, but $\text{patch}_{\text{allo}}$ with *Strategy-Major* did not work so well.

9.2.2.2. Writer Identification by Auto-derived Features on D_{uc} .

In Table 8, we present the 9-tuple writer identification accuracies of auto-derived feature-based models performing on the D_{uc} database.

Here also, from Table 8, we note that performance on the intra-variable handwritten sample with different training and testing sample types is not so well, i.e., AE_{smv} , AE_{sfv} , AE_{mfv} accuracies are comparatively low. The model XN_allo_mean produces the best outcome. The other model rankings can be observed in the rightmost column of Table 8. In this case, it can be noted that the overall *Strategy-Mean* worked better than the *Strategy-Major*.

Comparing Tables 7 and 8, it can be observed that the general performance on database D_c is better than D_{uc} . The rank orders are almost similar in cases of Tables 7 and 8. Here, only the ranks of model VN_char_major and VN_allo_major are interchanged. This scenario suggests that our model is quite stable for different databases.

All the auto-derived feature-based models worked better than handcrafted feature-based models. However, the AE_{smv} , AE_{sfv} , AE_{mfv} accuracies are also low here in comparison with the other accuracies of the 9-tuple. Using auto-derived features, the Top-2 (Top-5) writer identification accuracies of AE_{smv} , AE_{sfv} , AE_{mfv} increased at most 1.56% (7.76%) and 1.35% (6.89%) for D_c and D_{uc} , respectively.

In Fig. 9 - Fig. 10, we present the radar plots of 9-tuple accuracies of writer identification shown in Tables 5 - 8.

9.3. Writer Verification Performance

In this section, we discuss writer verification performances of the models employed using both handcrafted features and auto-derived features.

The writer verification accuracies are obtained as mentioned in Section 8. Similar to writer identification, here we also use multiple experimental setups and finally obtain 9-tuple accuracies (refer to Section 9.2.1). The *Borda count* [48] is also used here to rank the models and shown in the last columns of Tables 9 - 12.

9.3.1. Writer Verification Performance with Handcrafted Features

Similar to the three writer identification models employing handcrafted features (refer to Section 9.2.1), here also we obtain three writer verification models. These writer ver-

Table 7. Top-1 writer identification performance using auto-derived features on D_c

	Model (WI- D_c)	9-tuple Accuracy (%)									Rank	
		AE_{ss}	AE_{mm}	AE_{ff}	AE_{smv}	AE_{sfv}	AE_{mfv}	$AE_{smf/s}$	$AE_{smf/m}$	$AE_{smf/f}$		
Basic	_CNN	BCNN_char_major	81.25	81.72	81.51	57.58	50.03	53.67	83.72	83.32	82.58	23
		BCNN_allo_major	81.78	81.48	81.09	58.25	48.92	53.35	84.16	82.35	81.89	24
		BCNN_char_mean	83.56	83.12	82.37	60.02	51.27	55.93	85.58	84.73	83.89	22
		BCNN_allo_mean	84.53	83.63	82.92	60.59	51.34	55.25	86.21	85.33	84.74	21
Squeeze	Net	SN_char_major	87.27	85.54	85.14	62.92	53.15	58.03	88.16	87.69	86.29	19
		SN_allo_major	86.75	84.55	85.37	62.25	52.71	57.35	87.25	85.56	87.02	20
		SN_char_mean	88.46	87.79	87.31	65.35	56.79	61.53	90.27	89.35	89.05	18
		SN_allo_mean	89.23	88.48	87.72	66.56	56.05	61.45	90.53	89.72	89.25	17
GoogLe	Net	GN_char_major	91.09	90.07	87.97	67.37	57.08	62.58	91.60	91.44	90.44	13
		GN_allo_major	90.29	90.16	87.48	66.28	56.68	61.42	90.81	90.79	90.07	16
		GN_char_mean	91.34	89.78	89.29	68.04	58.28	63.99	92.58	90.62	91.20	12
		GN_allo_mean	91.39	90.48	90.04	69.12	58.92	63.24	93.13	92.16	91.25	11
VGG	-16	VN_char_major	91.02	89.25	88.58	67.33	57.53	62.22	91.71	90.03	90.43	15
		VN_allo_major	90.62	89.57	88.48	66.76	57.80	62.26	91.49	90.73	90.51	14
		VN_char_mean	91.91	91.24	90.47	68.27	59.13	64.17	92.53	92.07	92.29	10
		VN_allo_mean	92.74	90.91	91.29	69.23	60.04	64.37	93.43	91.89	92.63	9
ResNet	-101	RN_char_major	92.01	92.43	91.76	69.27	59.66	65.24	93.62	92.97	92.86	7
		RN_allo_major	92.44	91.72	91.05	69.69	59.61	64.98	93.42	92.33	92.27	8
		RN_char_mean	93.26	93.49	92.83	70.99	61.34	66.21	94.51	93.77	94.42	6
		RN_allo_mean	94.07	93.66	92.93	71.32	61.63	66.42	95.25	94.72	94.34	5
Xception	Net	XN_char_major	95.56	94.53	93.73	71.47	62.51	67.54	95.51	95.73	94.82	3
		XN_allo_major	94.83	93.66	93.50	70.93	62.58	66.83	95.07	95.19	94.48	4
		XN_char_mean	96.73	95.46	95.12	72.75	63.74	68.66	97.04	96.97	96.12	2
		XN_allo_mean	97.02	95.71	95.47	73.74	64.12	68.94	97.87	96.46	96.84	1

Table 8. Top-1 writer identification performance using auto-derived features on D_{uc}

		Model ($W_{I}D_{uc}$)	9-tuple Accuracy (%)								Rank	
			AE_{ss}	AE_{mm}	AE_{ff}	AE_{smv}	AE_{sfv}	AE_{mfv}	$AE_{smf/s}$	$AE_{smf/m}$		$AE_{smf/f}$
Basic	CNN	BCNN_char_major	80.69	80.53	80.43	56.26	47.65	52.59	82.19	80.77	80.72	23
		BCNN_allo_major	79.57	79.94	79.31	57.10	48.98	52.33	82.65	81.38	80.49	24
		BCNN_char_mean	81.96	82.05	82.78	58.16	49.47	53.04	84.22	83.23	82.01	22
SqueezeNet	Net	BCNN_allo_mean	83.01	81.73	81.64	59.5	50.02	54.15	85.13	84.24	82.81	21
		SN_char_major	86.06	83.91	83.93	60.88	51.78	56.81	86.47	86.13	85.11	19
		SN_allo_major	85.25	83.51	83.29	62.26	50.96	55.71	86.13	85.43	83.85	20
GoogLe	Net	SN_char_mean	88.12	86.82	86.78	63.80	54.45	58.53	89.48	89.25	88.98	18
		SN_allo_mean	89.33	88.03	87.06	65.27	54.84	60.17	90.57	89.54	88.57	17
		GN_char_major	90.31	89.96	87.82	66.14	55.75	60.79	90.85	91.34	89.82	13
VGG	-16	GN_allo_major	89.77	88.83	86.96	64.45	55.73	61.51	90.15	89.93	89.09	16
		GN_char_mean	90.43	90.47	88.39	66.41	56.48	60.86	92.14	90.79	91.07	12
		GN_allo_mean	90.54	89.46	89.24	67.39	57.59	61.94	91.82	91.41	90.45	11
ResNet	-101	VN_char_major	90.37	89.55	87.51	65.67	55.82	60.54	91.49	90.69	90.52	14
		VN_allo_major	89.74	88.85	88.63	66.92	55.64	60.41	91.61	89.20	90.41	15
		VN_char_mean	91.60	90.18	90.38	67.09	57.39	63.12	90.78	90.49	91.65	10
Xception	Net	VN_allo_mean	92.69	90.34	90.55	67.94	58.46	63.02	92.52	91.55	91.46	9
		RN_char_major	91.82	92.72	90.28	68.16	58.95	63.42	93.16	92.96	92.35	7
		RN_allo_major	91.85	91.42	90.73	68.60	57.41	63.07	92.42	91.41	91.97	8
ResNet	-101	RN_char_mean	92.72	93.38	92.27	69.03	60.02	64.64	93.79	93.01	93.57	6
		RN_allo_mean	94.13	93.42	92.36	69.45	59.63	65.13	94.47	94.21	93.48	5
		XN_char_major	95.13	94.31	92.82	69.15	60.89	65.77	95.27	95.34	93.85	3
Xception	Net	XN_allo_major	94.62	93.01	92.51	69.95	61.51	65.78	94.42	94.84	94.16	4
		XN_char_mean	96.49	94.56	94.56	70.85	61.85	67.81	96.25	96.04	95.74	2
		XN_allo_mean	96.81	95.52	95.03	72.52	62.79	66.53	97.09	96.59	95.62	1

ification models are experimented on both the databases D_c and D_{uc} . The procedure of model accuracy computation is described in Section 8.1. The performance of the models is discussed as follows.

9.3.1.1. Writer Verification by Handcrafted Features on D_c .

We have obtained WV_{D_c-FMM} , WV_{D_c-FDH} , WV_{D_c-FDC} models for writer verification similar to the writer identification models (refer to Section 9.2.1.1). For example, WV_{D_c-FMM} is such a writer verification model, where F_{MM} handcrafted features are used on database D_c .

In Table 9, we present the writer verification performance of these three models in terms of 9-tuple accuracy. The ranks of these models are mentioned in the rightmost column of Table 9. Here, the model WV_{D_c-FDH} performed best.

Table 9. Writer verification performance using handcrafted features on D_c

Model	9-tuple Accuracy (%)									Rank
	AE_{ss}	AE_{mm}	AE_{ff}	AE_{smv}	AE_{sfv}	AE_{mfv}	$AE_{smf/s}$	$AE_{smf/m}$	$AE_{smf/f}$	
WV_{D_c-FMM}	72.07	71.15	69.92	48.50	36.58	41.43	73.66	73.12	71.34	3
WV_{D_c-FDH}	86.64	86.06	85.69	53.72	43.57	48.18	87.87	87.57	86.02	1
WV_{D_c-FDC}	83.60	82.85	82.48	52.46	41.09	46.08	84.85	84.21	82.80	2

9.3.1.2. Writer Verification by Handcrafted Features on D_{uc} .

Here also, we have generated three handcrafted feature-based writer verification models $WV_{D_{uc}-FMM}$, $WV_{D_{uc}-FDH}$, $WV_{D_{uc}-FDC}$ for experimentation on database D_{uc} .

In Table 10, the writer verification results of these three models are presented, where the rightmost column shows their ranking. In this case, the model $WV_{D_{uc}-FDH}$ performed best.

For experimentation on both databases D_c and D_{uc} , the rankings are similar when using the same feature-based model. Overall, the F_{DH} feature-based model performed best and the F_{MM} feature-based model achieved lowest results for verification also.

Table 10. Writer verification performance using handcrafted features on D_{uc}

Model	9-tuple Accuracy (%)									Rank
	AE_{ss}	AE_{mm}	AE_{ff}	AE_{smv}	AE_{sfv}	AE_{mfv}	$AE_{smf/s}$	$AE_{smf/m}$	$AE_{smf/ff}$	
$WV_{D_{uc}}-FMM$	69.58	69.05	67.09	47.96	35.76	40.26	71.43	70.12	69.34	3
$WV_{D_{uc}}-FDH$	84.87	84.45	84.52	52.34	40.88	46.50	86.20	86.24	84.03	1
$WV_{D_{uc}}-FDC$	81.50	80.38	81.12	50.86	39.32	45.74	83.09	83.05	81.34	2

It can be observed from Tables 9 and 10 that the accuracies AE_{smv} , AE_{sfv} , AE_{mfv} are very low in comparison with other accuracies of 9-tuple. Here, the ranks in Tables 9 and 10 are the same for similar handcrafted feature-based models employed in D_c and D_{uc} .

9.3.2. Writer Verification Performance with Auto-derived Features

In this section, we discuss the performance of auto-derived feature-based writer verification models. The procedure to obtain the verification accuracy using auto-derived features is mentioned in Section 8.2. Here, only the *Strategy-Mean* is used, since the *Strategy-Major* performed insignificantly. Therefore, we have obtained 12 models from 6 types of convolutional networks, with 2 forms of patch (patch_{char} and patch_{allo}), fed using only one strategy. The naming convention of these verification models is kept similar to the writer identification models.

9.3.2.1. Writer Verification by Auto-derived Features on D_c .

In Table 11, we present the 9-tuple writer verification accuracies using auto-derived features while experimenting on D_c . Here, XN_allo_mean performed best. All the model rankings are presented in the rightmost column of Table 11. In general, patch_{allo} worked better than patch_{char}. Only for VGG-16, the patch_{char} performed better than patch_{allo}.

Table 11. Writer verification performance using auto-derived features on D_c

Model (WV_{D_c})	9-tuple Accuracy (%)									Rank
	AE_{ss}	AE_{mm}	AE_{ff}	AE_{smv}	AE_{sfv}	AE_{mfv}	$AE_{smf/s}$	$AE_{smf/m}$	$AE_{smf/ff}$	
BCNN_char_mean	92.22	91.48	92.13	69.19	60.94	66.59	94.17	93.53	93.44	12
BCNN_allo_mean	92.45	91.78	92.75	70.69	61.84	66.28	93.33	92.12	92.72	11
SN_char_mean	95.74	94.85	95.53	74.85	65.14	70.97	97.24	97.31	96.55	10
SN_allo_mean	96.09	95.09	96.52	77.08	66.16	70.75	96.53	95.93	96.07	9
GN_char_mean	96.55	95.60	96.21	75.39	65.97	71.42	97.97	97.97	96.73	8
GN_allo_mean	96.24	95.83	96.55	77.90	66.18	71.47	97.38	96.79	96.58	7
VN_char_mean	97.77	96.36	97.02	75.80	66.69	72.19	98.39	98.17	97.67	5
VN_allo_mean	97.20	96.81	96.73	78.04	66.48	72.35	97.82	96.96	97.08	6
RN_char_mean	98.21	97.85	98.24	77.48	67.83	73.28	99.50	99.47	99.05	4
RN_allo_mean	98.74	98.15	98.27	79.72	68.36	73.51	99.76	98.73	98.95	3
XN_char_mean	98.95	98.79	98.82	78.68	69.70	75.24	99.76	99.68	99.27	2
XN_allo_mean	99.24	99.06	98.68	80.79	70.02	74.98	99.84	99.73	99.18	1

9.3.2.2. Writer Verification by Auto-derived Features on D_{uc} .

On database D_{uc} , the 9-tuple writer verification accuracies of various auto-derived feature-based models are shown in Table 12. In this case, XN_allo_mean performed best. The ranks of other models are shown in the rightmost column of Table 12. Overall, patch_{allo} worked better than patch_{char} except for VGG-16 and GoogLeNet.

From Tables 11 and 12, it can be observed that the AE_{smv} , AE_{sfv} , AE_{mfv} accuracies are very low in comparison with other accuracies of 9-tuple. Here, Tables 11 and 12 depict similar ranks except for the GoogLeNet-based models.

Table 12. Writer verification performance using auto-derived features on D_{uc}

Model ($WV_{D_{uc}}$)	9-tuple Accuracy (%)									Rank
	AE_{ss}	AE_{mm}	AE_{ff}	AE_{smv}	AE_{sfv}	AE_{mfv}	$AE_{smf/s}$	$AE_{smf/m}$	$AE_{smf/f}$	
BCNN_char_mean	91.55	90.57	91.26	69.15	60.17	65.54	93.24	92.57	92.06	12
BCNN_allo_mean	91.78	90.92	91.78	70.29	61.31	65.91	92.63	91.81	92.53	11
SN_char_mean	95.36	94.25	94.54	74.77	64.15	69.98	96.50	96.95	96.12	10
SN_allo_mean	95.86	94.46	96.50	76.84	65.35	70.54	96.06	95.90	95.47	9
GN_char_mean	95.86	95.29	96.02	74.95	65.36	71.27	97.07	97.09	96.67	7
GN_allo_mean	95.55	95.29	96.54	77.14	65.81	70.52	97.23	96.76	96.12	8
VN_char_mean	97.36	96.02	96.72	75.10	66.58	71.62	97.06	97.94	97.62	5
VN_allo_mean	96.43	96.75	95.99	77.28	66.18	72.34	97.67	96.61	96.45	6
RN_char_mean	97.46	97.63	98.02	77.15	67.22	73.03	99.30	99.29	98.53	4
RN_allo_mean	98.44	98.03	98.27	79.40	68.26	73.37	98.89	97.79	98.13	3
XN_char_mean	98.73	98.69	98.06	78.13	69.29	74.28	99.65	98.96	98.77	2
XN_allo_mean	98.55	98.73	97.89	79.84	69.80	74.76	99.19	99.54	98.54	1

In Fig. 11 - Fig. 12, we present the radar plots of 9-tuple accuracies of writer verification shown in Tables 9 - 12.

9.4. Observations

From the above experiments (refer to Sections 9.2 and 9.3, Tables 5 - 12, Fig. 9 - Fig. 12), our major observations are noted as follows:

i) Among the accuracies in 9-tuple, the AE_{smv} , AE_{sfv} , AE_{mfv} accuracies are comparatively low for all the models used for *writer identification/verification*. It suggests that if the training and test set contain similar types of samples, the models can perform better.

Moreover, here the AE_{sfv} accuracy is lower than AE_{smv} and AE_{mfv} . It indicates that sets S_s and S_f of D_c (S'_s and S'_f sets of D_{uc}) contain higher intra-variable writing than the other set combinations.

ii) The auto-derived features worked better than the handcrafted features for the *writer identification/verification*. The reason may be the high dimensionality of the auto-derived features and the use of deep convolutional architectures.

Among the handcrafted features, F_{DH} performed best, while F_{DC} performed better than F_{MM} . Among auto-derived features, Xception Net-based features worked best.

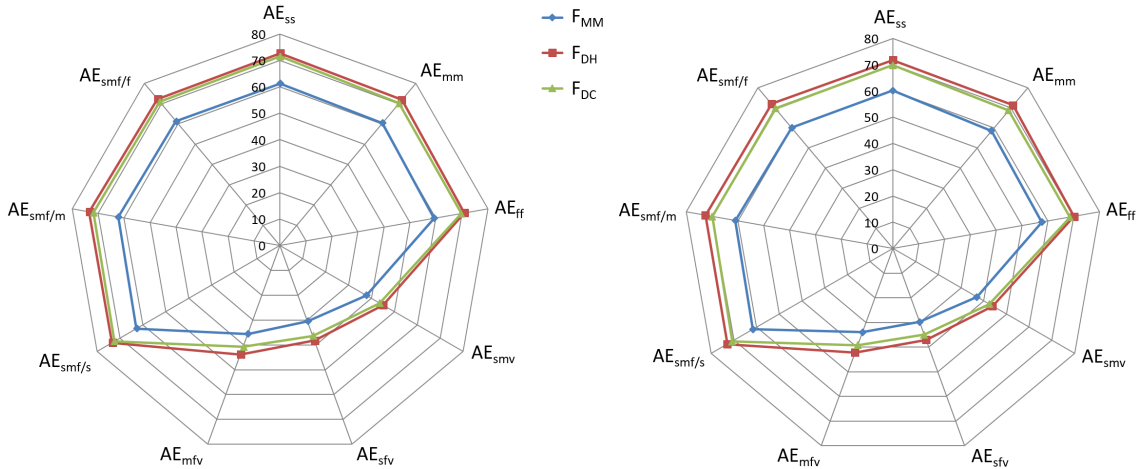


Figure 9: Radar plot of Top-1 writer identification performance using handcrafted features. *Left*: representing Table 5 on D_c and *Right*: representing Table 6 on D_{uc} .

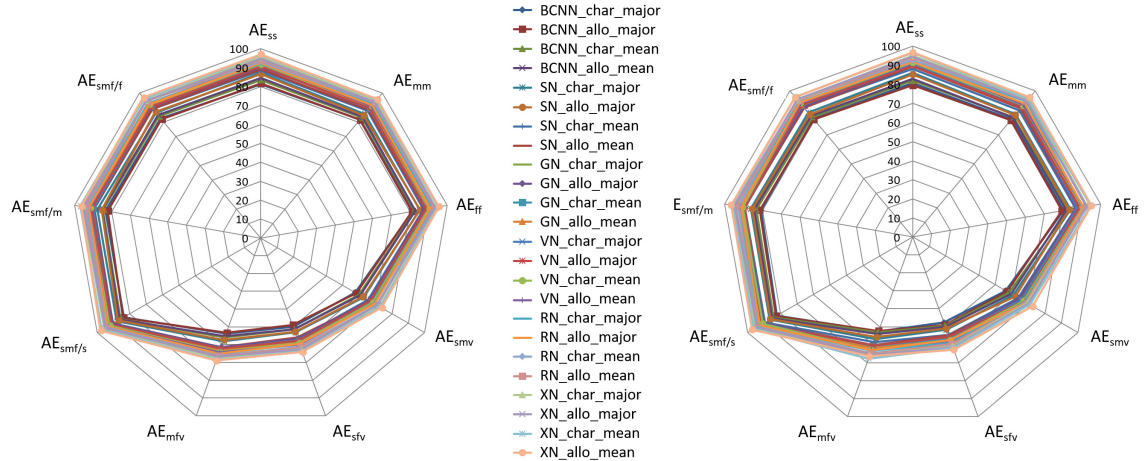


Figure 10: Radar plot of Top-1 writer identification performance using auto-derived features. *Left*: representing Table 7 on D_c and *Right*: representing Table 8 on D_{uc} .

iii) For auto-derived feature-based *writer identification* models, mostly the *Strategy-Mean* worked better than *Strategy-Major*.

iv) In general, for auto-derived feature-based *writer identification* models, $\text{patch}_{\text{allo}}$ with *Strategy-Mean* worked best, whereas $\text{patch}_{\text{allo}}$ with *Strategy-Major* performed lowest. Combining $\text{patch}_{\text{char}}$, *Strategy-Mean* worked better than *Strategy-Major*. In other words, using combinations of *patch* and *Strategy*, the overall performance in highest to lowest order is as follows: $\text{allo_mean} \succ \text{char_mean} \succ \text{char_major} \succ \text{allo_major}$.

v) For auto-derived feature-based *writer verification* models, mostly the $\text{patch}_{\text{allo}}$ worked better than the $\text{patch}_{\text{char}}$.

vi) All together, the *writer identification/verification* performance on the controlled database (D_c) is better than the uncontrolled database (D_{uc}).

vii) As a whole, all the *writer identification/verification* models provide quite similar AE_{ss} , AE_{mm} , AE_{ff} accuracies (differences range up to 3.12% Top-1). This implies that our system is quite robust on working with various handwriting types.

viii) In general, the handcrafted feature-based models and auto-derived feature-based models for *writer identification/verification* follow the same trend, respectively (refer to Tables 5 - 12). It can be visualized by the radar plots of Fig. 9 - Fig. 12. Here, the individual radar plot follows almost the same trend with creating a band of certain width.

9.5. Writer Identification/Verification by Pre-training

From the previous experiments, we have observed that AE_{smv} , AE_{sfv} , AE_{mfv} accuracies are relatively lower than other accuracies of the 9-tuple. Therefore, in this section, we aim to increase these three accuracies (AE_{smv} , AE_{sfv} , AE_{mfv}), say, by 3-tuple.

We have noted that the auto-derived features worked better than the handcrafted features. Therefore, here we focus only on auto-derived features. We have also observed that the *Xception Net* performed best among all models for our problem. Hence, we continue investigations with this network for increasing the 3-tuple (AE_{smv} , AE_{sfv} , AE_{mfv}) accuracies, and present them here and further in this paper.

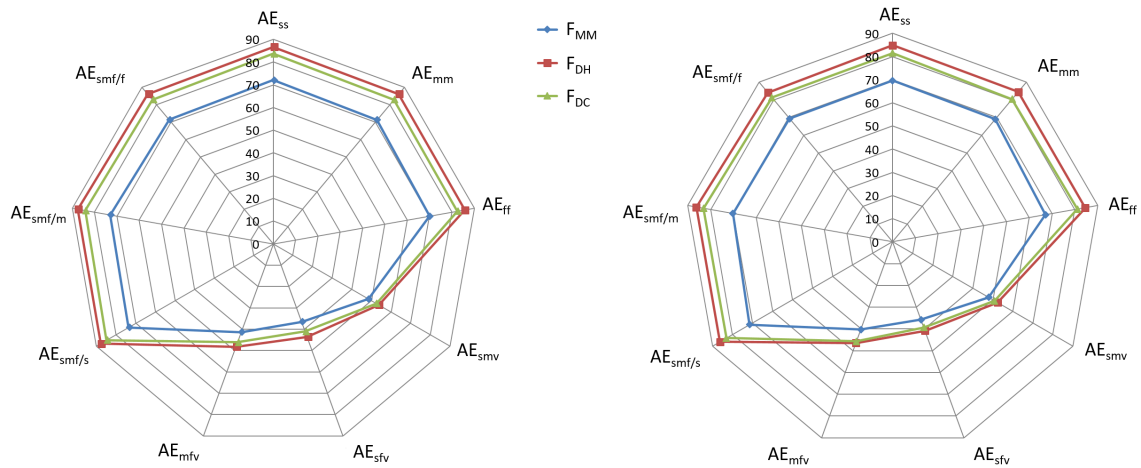


Figure 11: Radar plot of writer verification performance using handcrafted features. *Left*: representing Table 9 on D_c and *Right*: representing Table 10 on D_{uc} .

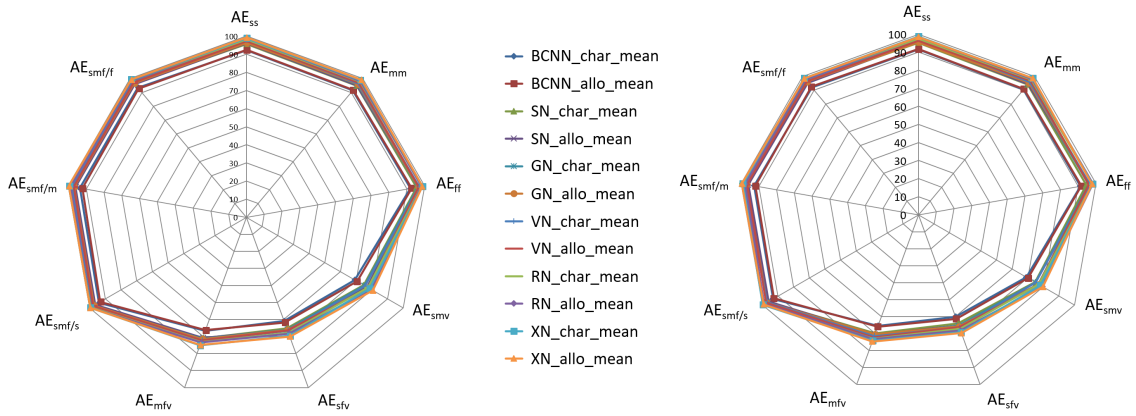


Figure 12: Radar plot of writer verification performance using auto-derived features. *Left*: representing Table 11 on D_c and *Right*: representing Table 12 on D_{uc} .

It can be reiterated that the 100 writers contributing to the D_c database are completely different from the 100 writers in D_{uc} . As a matter of fact, there is no writer overlap between D_c and D_{uc} (refer to Section 3.2).

We pre-train the model using D_{uc} and repeat our experiments on D_c (say, $E_{D_{uc}}/D_c$). We get this idea from the *transfer learning* approach [57]. For pre-training, the total database D_{uc} is used. Then previous experimental setups, i.e., E_{sm} , E_{ms} , E_{sf} , E_{fs} , E_{mf} and E_{fm} , are used to obtain AE_{smv} , AE_{sfv} , AE_{mfv} accuracies (refer to Section 9.2). For example, we have pre-trained the model using all the data of D_{uc} , now for the E_{sm} setup, we again train the model with S_{s1} and test on S_{m3} .

Likewise, the E_{D_c}/D_{uc} experiment is performed where the total D_c is used for pre-training, and then the earlier experiments are repeated on D_{uc} (refer to Section 9.2, 9.3). Here, two databases have assisted each other in pre-training/learning to study the system performance. Such a technique may be referred to as *cross-learning*.

In Table 13, we present the Top-1 *writer identification* performances on $E_{D_{uc}}/D_c$ and

E_{D_c}/D_{uc} experimental setups employing various *Xception Net* models.

From Table 13, it can be observed that substantially the XN_allo_mean performed best for both $E_{D_{uc}}/D_c$ and E_{D_c}/D_{uc} setups. Overall, on 3-tuple accuracy, the highest-to-lowest performance order is as follows: XN_allo_mean \succ XN_char_mean \succ XN_char_major \succ XN_allo_major. The only exception is to obtain AE_{mfv} accuracy in $E_{D_{uc}}/D_c$, where the XN_allo_major worked better than XN_char_major.

Overall, for $E_{D_{uc}}/D_c$ and E_{D_c}/D_{uc} experiments, the Top-2 (Top-5) writer identification criteria produced up to 1.86% (7.52%) and 2.08% (8.37%) additional accuracy, respectively.

The *writer verification* performance for the experimental setups $E_{D_{uc}}/D_c$ and E_{D_c}/D_{uc} are presented in Table 14. Here, for both the $E_{D_{uc}}/D_c$ and E_{D_c}/D_{uc} experiments, mostly patch_{allo} worked better than patch_{char}. The only exception is to obtain AE_{smv} in E_{D_c}/D_{uc} where XN_char_mean worked better than XN_allo_mean.

Compared to the results of Section 9.2 and 9.3, here it can be seen that such pre-training with cross-learning has improved the system performance (at most 5.23% for identification and 3.00% for verification).

Now, comparing the experimental setups of Tables 13 and 14, we observe that $E_{D_{uc}}/D_c$ performed better than E_{D_c}/D_{uc} for both identification and verification. Here also, all the models/experimental setups are compared using the *Borda count* [48].

9.6. Writer Identification/Verification on the Enlarged Writer Set

In this section, we would like to see the system performance on an increased number of writers. For this purpose, we merged the controlled (D_c) and uncontrolled (D_{uc}) databases and get data from 200 writers. This experimental setup is denoted as $E_{D_{c+uc}}$.

Here also, we show the 3-tuple accuracies of *Xception Net*-based models as in Section 9.5, although we have computed 9-tuple accuracies from all models (refer to Section 9.2, 9.3).

The earlier experimental setups, i.e., E_{sm} , E_{ms} , E_{sf} , E_{fs} , E_{mf} and E_{fm} setups, are used here to obtain AE_{smv} , AE_{sfv} , AE_{mfv} accuracies (refer to Section 9.2). For example, the setup E_{sm} of $E_{D_{c+uc}}$ is trained by the $S_{s1} + S'_{s1}$ set and is tested on the $S_{m3} + S'_{m3}$ set.

In Table 15, we present the Top-1 *writer identification* performance in terms of 3-tuple accuracy, which shows that XN_allo_mean performed best. Overall, on 3-tuple accuracy, the performance from highest to lowest order is as follows: XN_allo_mean \succ XN_char_mean \succ XN_char_major \succ XN_allo_major. However, there is an exception for AE_{sfv} where XN_allo_major has worked better than XN_char_major.

Overall for $E_{D_{c+uc}}$, the Top-2 and Top-5 writer identification criteria produced up to 0.47% and 4.38% additional accuracies, respectively.

Table 13. Top-1 writer identification by pre-training

Setup	Model (WI)	3-tuple Accuracy (%)			Setup	Model (WI)	3-tuple Accuracy (%)		
		AE_{smv}	AE_{sfv}	AE_{mfv}			AE_{smv}	AE_{sfv}	AE_{mfv}
$E_{D_{uc}}/D_c$	XN_char_major	74.68	63.92	68.09	E_{D_c}/D_{uc}	XN_char_major	74.03	63.89	67.75
	XN_allo_major	73.64	63.38	68.47		XN_allo_major	72.78	63.24	67.54
	XN_char_mean	76.31	66.38	71.03		XN_char_mean	75.70	65.41	70.87
	XN_allo_mean	77.37	67.21	71.95		XN_allo_mean	76.57	66.56	71.76

Table 14. Writer verification by pre-training

Setup	Model (WV)	3-tuple Accuracy (%)		
		AE_{smv}	AE_{sfv}	AE_{mfv}
E_D_{uc}/D_c	XN_char_mean	83.05	72.21	76.82
	XN_allo_mean	83.54	72.45	77.65
E_D_c/D_{uc}	XN_char_mean	82.58	71.69	76.25
	XN_allo_mean	82.34	72.47	77.76

Table 15. Top-1 writer identification on enlarged writer set

Model (W E_Dc+uc)	3-tuple Accuracy (%)		
	AE_{smv}	AE_{sfv}	AE_{mfv}
XN_char_major	73.96	63.84	67.27
XN_allo_major	72.72	64.02	67.16
XN_char_mean	76.07	66.37	70.79
XN_allo_mean	77.76	66.72	70.95

In Table 16, we present the *writer verification* performance of the E_D_{c+uc} setup. In this case, XN_allo_mean worked better than XN_char_mean.

Table 16. Top-1 writer verification on an enlarged writer set

Model (WV-E_Dc+uc)	3-tuple Accuracy (%)		
	AE_{smv}	AE_{sfv}	AE_{mfv}
XN_char_mean	83.68	72.65	77.19
XN_allo_mean	84.02	72.81	77.87

For writer identification/verification on E_D_{c+uc} , XN_allo_mean performed best. Here, all the models are compared using *Borda count* [48].

By comparing with the results from Sections 9.2 and 9.3, we see that the system performance has slightly increased (at most 4.02% for identification and 3.23% for verification) with the number of writers.

9.7. Comparison with Other Works

To the best of our knowledge and understanding, our work is the earliest attempt of its kind on such a problem. Also, we did not find any other published research work on this topic to be compared.

10. Conclusion

In this paper, we work on writer identification/verification when there is extensive variation in a person’s handwriting. In brief, we focus on high intra-variable handwriting-based writer investigation. We employ both handcrafted and auto-derived feature-based models to study writer identification/verification performance. We generated two offline Bengali intra-variable handwriting databases from two different sets of 100 writers. For this database generation, we have also worked with auto-derived feature-based grouping technique to form similar groups of intra-variable writing. After experimenting on our databases, we observe that by training and testing on similar writing variability, our system produces encouraging outcomes. However, our system performance is comparatively lower for training and testing on disparate types of handwriting variability. We also attempt with cross-learning and see that the system performance improves with pre-training.

Here, a practical scenario is imitated, whereby a certain writing style of an individual is unknown (i.e., absent during training), and we note that the state-of-the-art methods do not perform well. However, we also observe that the deep features have high potential for

this task. In future, we will try to exploit this potential and find some latent characteristics of a person from his/her varying styles of writing.

Acknowledgment

We heartily thank all the volunteers for their immense help in generating our database.

References

- [1] A. Brink, H. van der Klauw, L. Schomaker, 2008. Automatic Removal of Crossed-Out Handwritten Text and the Effect on Writer Verification and Identification. DRR, XV, #68150A.
- [2] A. Fahad et al., 2014. A Survey of Clustering Algorithms for Big Data: Taxonomy and Empirical Analysis. IEEE Trans. on Emerging Topics in Computing 2 (3), 267–279.
- [3] A. Gordo, A. Forns, E. Valveny, 2013. Writer Identification in Handwritten Musical Scores with Bags of Notes. Pattern Recognition 46 (5), 1337–1345.
- [4] A. Krizhevsky, I. Sutskever, G. E. Hinton, 2012. ImageNet Classification with Deep Convolutional Neural Networks. Proc. Int. Conf. on Neural Information Processing Systems (NIPS) 1, 1097–1105.
- [5] A. L. Wong, A. M. Haith, J. W. Krakauer, 2015. Motor Planning. Neuroscientist 21 (4), 385–398.
- [6] A. M. Wing, A. D. Baddeley, 1978. A Simple Measure of Handwriting as an Index of Stress. Bulletin of the Psychonomic Society 11 (4), 245–246.
- [7] A. Naftali, 1965. Behavior Factors in Handwriting Identification. The Journal of Criminal Law, Criminology and Police Science 56 (4), 528–539.
- [8] A. Schlapbach, H. Bunke, 2005. Writer Identification using an HMM-based Handwriting Recognition System: To Normalize the Input or Not? Conference of the IGS, 138–142.
- [9] B. B. Chaudhuri, C. Adak, 2017. An Approach for Detecting and Cleaning of Struck-out Handwritten Text. Pattern Recognition 61, 282–294.
- [10] B. B. Chaudhuri, U. Pal, 1998. A Complete Printed Bangla OCR System. Pattern Recognition 31 (5), 531–549.
- [11] B. McCune, J. B. Grace, 2002. Analysis of Ecological Communities. MjM Software, Gleneden Beach, Oregon, USA, Ch. 6.
- [12] C. Adak, B. B. Chaudhuri, 2013. Extraction of Doodles and Drawings from Manuscripts. Int. Conf. on Pattern Recognition and Machine Intelligence (PReMI), LNCS #8251, 515–520.
- [13] C. Adak, B. B. Chaudhuri, 2015. Writer Identification from Offline Isolated Bangla Characters and Numerals. ICDAR, 486–490.
- [14] C. Adak, B. B. Chaudhuri, M. Blumenstein, 2016. Writer Identification by Training on One Script but Testing on Another. Int. Conference on Pattern Recognition (ICPR), 1148–1153.
- [15] C. Adak, B. B. Chaudhuri, M. Blumenstein, 2017. Impact of Struck-out Text on Writer Identification. IJCNN, 1465–1471.
- [16] C. D. Manning, P. Raghavan, H. Schtze, 2008. Introduction to Information Retrieval. Cambridge University Press.
- [17] C. Djeddi, I. Siddiqi, L. S.- Meslati, A. Ennaji, 2013. Text-Independent Writer Recognition Using Multi-Script Handwritten Texts. Pattern Recognition Letters 34 (10), 1196–1202.
- [18] C. L. Liu, C. Y. Suen, 2009. A New Benchmark on the Recognition of Handwritten Bangla and Farsi Numeral Characters. Pattern Recognition 42 (12), 3287–3295.
- [19] C. Szegedy et al., 2014. Going Deeper with Convolutions. arXiv:1409.4842.

- [20] C. Szegedy, V. Vanhoucke, S. Ioffe, J. Shlens, Z. Wojna, 2015. Rethinking the Inception Architecture for Computer Vision. arXiv:1512.00567.
- [21] E. Ahmed, M. Jones, T. K. Marks, 2015. An Improved Deep Learning Architecture for Person Re-identification. CVPR, 3908–3916.
- [22] F. Aiciolu, N. Turan, 2003. Handwriting Changes Under the Effect of Alcohol. Forensic Science International 132 (3), 201–210.
- [23] F. Chollet, 2016. Xception: Deep Learning with Depthwise Separable Convolutions. arXiv:1610.02357v3.
- [24] F. N. Iandola, S. Han, M. W. Moskewicz, K. Ashraf, W. J. Dally, K. Keutzer, 2016. SqueezeNet: AlexNet-level Accuracy with 50x Fewer Parameters and <0.5 MB Model Size. arXiv:1602.07360.
- [25] F. Zhao, H. Z. Lu, Z. Y. Zhang, 2013. Real-time Single-pass Connected Components Analysis Algorithm. EURASIP Journal on Image and Video Processing 21, 1–10.
- [26] G. E. Hinton, N. Srivastava, A. Krizhevsky, I. Sutskever, R. R. Salakhutdinov, 2012. Improving Neural Networks by Preventing Co-Adaptation of Feature Detectors. arXiv: 1207.0580.
- [27] H. Kameya, S. Mori, R. Oka, 2003. Figure-Based Writer Verification by Matching between an Arbitrary Part of Registered Sequence and an Input Sequence Extracted from On-Line Handwritten Figures. ICDAR, 985–989.
- [28] J. Behrendt, 1984. Alzheimer’s Disease and Its Effect on Handwriting. Journal of Forensic Sciences 29 (1), 87–91.
- [29] J. Bromley, I. Guyon, Y. LeCun, E. Sckinger, R. Shah, 1993. Signature Verification using a “Siamese” Time Delay Neural Network. NIPS, 737–744.
- [30] J. Chen, D. Lopresti, G. Nagy, 2016. Conservative Preprocessing of Document Images. IJDAR 19 (4), 321–333.
- [31] J. Mathyer, 1969. The Influence of Writing Instruments on Handwriting and Signatures. The Journal of Criminal Law, Criminology and Police Science 60 (1), 102–112.
- [32] J. Michell, 1996. Who Wrote Shakespeare? Thames and Hudson Ltd., London.
- [33] J. Milgram, M. Cheriet, R. Sabourin, 2006. “One Against One” or “One Against All”: Which One is Better for Handwriting Recognition with SVMs? Proc. Int. Workshop on Frontiers in Handwriting Recognition (IWFHR).
- [34] J. Neyman, E. Pearson, 1933. On the Problem of the Most Efficient Tests of Statistical Hypotheses. Philosophical Transactions of the Royal Society of London, series A 231, 289–337.
- [35] J. Walton, 1997. Handwriting Changes Due to Aging and Parkinson’s Syndrome. Forensic Science International 88 (3), 197–214.
- [36] K. Amend, M. S. Ruiz, 1980. Handwriting Analysis: The Complete Basic Book. The Career Press, NJ 07417.
- [37] K. Duan, S. S. Keerthi, A. N. Poo, 2003. Evaluation of Simple Performance Measures for Tuning SVM Hyperparameters. Neurocomputing 51, 41–59.
- [38] K. He, X. Zhang, S. Ren, J. Sun, 2016. Deep Residual Learning for Image Recognition. Proc. CVPR, 770–778.
- [39] K. M. Koppenhaver, 2007. Factors That Cause Changes in Handwriting. Humana Press, New Jersey, Ch. 3 of Forensic Document Examination: Principles and Practice, pp. 27–36.
- [40] K. Simonyan, A. Zisserman, 2014. Very Deep Convolutional Networks for Large-Scale Image Recognition. arXiv:1409.1556.
- [41] L. Lam, S. W. Lee, C. Y. Suen, 1992. Thinning Methodologies - A Comprehensive Survey. IEEE Trans. on PAMI 14 (9), 869–885.
- [42] L. Nanni, S. Ghidoni, S. Brahmam, 2017. Handcrafted vs. Non-Handcrafted Features for Computer Vision Classification. Pattern Recognition 71, 158–172.
- [43] M. Bulacu, L. Schomaker, 2007. Text-Independent Writer Identification and Verification Using Textural and Allographic Features. IEEE Trans. on PAMI 29 (4), 701–717.

- [44] M. Z. Alom et al., 2018. The History Began from AlexNet: A Comprehensive Survey on Deep Learning Approaches. arXiv:1803.01164.
- [45] N. Stamatopoulos et al., 2013. ICDAR 2013 Handwriting Segmentation Contest. ICDAR, 1402–1406.
- [46] O. Hilton, 1984. Effects of Writing Instruments on Handwriting Details. *Journal of Forensic Sciences* 29 (1), 80–86.
- [47] O. Russakovsky et al., 2015. ImageNet Large Scale Visual Recognition Challenge. *IJCV* 115 (3), 211–252.
- [48] P. Emerson, 2013. The Original Borda Count and Partial Voting. *Social Choice and Welfare* 40 (2), 353–358.
- [49] R. D. Banerji, 1919. The Origin of the Bengali Script. University of Calcutta.
- [50] R. Hadsell, S. Chopra, Y. LeCun, 2006. Dimensionality Reduction by Learning an Invariant Mapping. *Proc. CVPR*, 1735–1742.
- [51] R. Plamondon, G. Lorette, 1989. Automatic Signature Verification and Writer Identification - The State of the Art. *Pattern Recognition* 22 (2), 107–131.
- [52] S. Chopra, R. Hadsell, Y. LeCun, 2005. Learning A Similarity Metric Discriminatively, with Application to Face Verification. *CVPR* 1, 539–546.
- [53] S. F. Bolich, 2009. History of Handwriting Analysis. Author House, Indiana, Ch. I of What America Lost: Decades that Made A Difference: Tracking Attitude Changes through Handwriting, pp. 1–4.
- [54] S. Gerth et al., 2016. Is Handwriting Performance Affected by the Writing Surface? Comparing Preschoolers, Second Graders, and Adults Writing Performance on a Tablet vs. Paper. *Frontiers in Psychology* 7, article no. 1308.
- [55] S. He, L. Schomaker, 2017. Writer Identification using Curvature-Free Features. *Pattern Recognition* 63, 451–464.
- [56] S. Ioffe, C. Szegedy, 2015. Batch Normalization: Accelerating Deep Network Training by Reducing Internal Covariate Shift. *Proc. Int. Conf. on Machine Learning (ICML)*, 448–456.
- [57] S. J. Pan, Q. Yang, 2010. A Survey on Transfer Learning. *IEEE Trans. on Knowledge and Data Engineering* 22 (10), 1345–1359.
- [58] S. Jaeger, S. Manke, J. Reichert, A. Waibel, 2001. Online Handwriting Recognition: The NPen++ Recognizer. *IJDAR* 3 (3), 169–180.
- [59] S. N. Srihari, S.- H. Cha, H. Arora, S. Lee, 2002. Individuality of Handwriting. *Journal of Forensic Sciences* 47 (4), 856–872.
- [60] T. Y. Lin, Y. Cui, S. Belongie, J. Hays, 2015. Learning Deep Representations for Ground-to-Aerial Geolocalization. *CVPR*, 5007–5015.
- [61] T. Y. Zhang, C. Y. Suen, 1984. A Fast Parallel Algorithm for Thinning Digital Patterns. *Commun. ACM* 27 (3), 236–239.
- [62] U. Pal, S. Datta, 2003. Segmentation of Bangla Unconstrained Handwritten Text. *ICDAR*, 1128–1132.
- [63] V. Christlein, D. Bernecker, A. Maier, E. Angelopoulou, 2015. Offline Writer Identification Using Convolutional Neural Network Activation Features. *German Conference on Pattern Recognition*, 540–552.
- [64] V. N. Vapnik, 2000. *The Nature of Statistical Learning Theory*. Springer-Verlag, New York.
- [65] V. Nair, G. E. Hinton, 2010. Rectified Linear Units Improve Restricted Boltzmann Machines. *Proc. ICML*, 807–814.
- [66] W. Yang, L. Jin, M. Liu, 2015. Chinese Character-level Writer Identification using Path Signature Feature, Dropstroke and Deep CNN. *Proc. ICDAR*, 546–550.
- [67] X. Wu, Y. Tang, W. Bu, 2014. Offline Text-Independent Writer Identification Based on Scale Invariant Feature Transform. *IEEE TIFS* 9 (3), 526–536.

- [68] Y.- J. Xiong, Y. Lu, P. S. P. Wang, 2017. Off-line Text-Independent Writer Recognition: A Survey. *Int. Journal of Pattern Recognition and Artificial Intelligence* 31 (5), #1756008 (32 pages).
- [69] Y. LeCun, L. Bottou, Y. Bengio, P. Haffner, 1998. Gradient-based Learning Applied to Document Recognition. *Proceedings of the IEEE* 86 (11), 2278–2324.
- [70] Y. Ma, G. Guo, 2014. *Support Vector Machines Applications*. Springer International Publishing, Switzerland.